Academic year
2023 - 2024

CFD simulations of two-phase flow in the manifold of a heat pump

Baptist Elst

Master's thesis
Master of Science in Electromechanical Engineering Technology

Supervisor
prof. dr. ir. Ilya T'Jollyn, UAntwerpen

Cosupervisor
Mitchell Whiting, EMIB, UAntwerpen

University of Antwerp
Faculty of Applied Engineering

Acknowledgements

As I approach the end of my studies as an engineer, I can look back on my student years with great happiness and satisfaction. This journey has been enriching, both personally and academically. This thesis represents the culmination of my studies.
When I started this major, I had far too little mathematical and technical background. To be honest, I never expected to make it this far. The challenges were demanding, but each challenge taught me valuable lessons.

First I would like to thank my supervisor, Ilya T'Jollyn, and my co-supervisor, Mitchell. Their invaluable insights and unwavering support have been crucial throughout the development of this master's thesis. Their expertise and guidance were essential in shaping my research and completing this work.

I am also extremely grateful to my parents for their constant encouragement and support. A special thank you goes to my girlfriend, Gitte, whose unending patience and motivation kept me going through the most challenging times of this thesis.
Additionally, I would like to express my appreciation to Lore for her assistance in checking my paper for language mistakes. Her help has been greatly appreciated and has significantly improved the quality of this thesis.

Abstract

In a heat pump, a two-phase refrigerant flows into the evaporator, which consists of several parallel tubes to limit pressure drop. The manifold, represented by an impacting T-junction, distributes the different phases across these tubes.
This thesis develops a 2D quasi-steady-state Computational Fluid Dynamics (CFD) model of an impacting T-junction with a horizontal inlet and vertical outlets to investigate the impact of various inlet parameters on the phase distribution.
The collision between the fluid and the junction wall leads to the formation of multiple droplets, which are modelled using the Volume Of Fluid (VOF) approach to achieve a sharp interface between the phases. After constructing the model, simulations were performed. In this way the influence of the mass flux and the vapour quality on the phase distribution of R410A were investigated, where an increasing mass flux was found to decrease the maldistribution of the two phases.
However, the influence of the vapour quality depended on the type of flow regime flowing through the junction. For the annular flows, increasing the vapour quality increased the maldistribution. The opposite was observed for the stratified wavy and intermittent flows. These findings were explained in terms of the various forces affecting the phase distribution.
At the end a general comparison across different flow regimes concludes that annular flows yield a more uniform distribution compared to stratified wavy flows.

Contents

List of Figures

Symbols

A_i	Area occupied by phase i
D	Tube diameter
E	Amount of liquid contained as droplets in the vapor core
F	Force
Fr	Froude number
G	Mass flux
g	Gravity acceleration
h	Gravity acceleration Enthalpy
J	Superficial velocity
L	Tube length
M_k	Momentum tranfer of phase k
$\dot{m}$	Mass flow rate
m_i	Mass of particle i
P	Pressure
Q	Heat
Re	Reynolds number
t	time
u	Velocity
$\dot{V}$	Volume flow rate
W	Work
We	Weber number

x	Vapour Quality
x_i	Location of particle i
σ	surface tension
θ	Inclination angle
ε	Void fraction
ρ	Density
μ	Dynamic viscosity

1 Introduction

In order to achieve the envisioned climate targets, the European Union and the Belgian government must implement a variety of energy saving measures. One of these measures is to support residents to install a heat pump. Considering the novelty of the heat pump technology, many optimisations could be performed to improve this technology. This thesis seeks to contribute to these optimisations, with the aim of advancing toward a more environmentally sustainable society.

A heat pump consists of several parts including the evaporator, compressor, condenser and the expansion valve, through which a refrigerant flows, as shown in Figure 1.1. This refrigerant is used to convert low temperature heat into high temperature heat using work. This causes the refrigerant to sequentially evaporate and condense. As a result, two phases exist together in multiple places inside the heat pump.

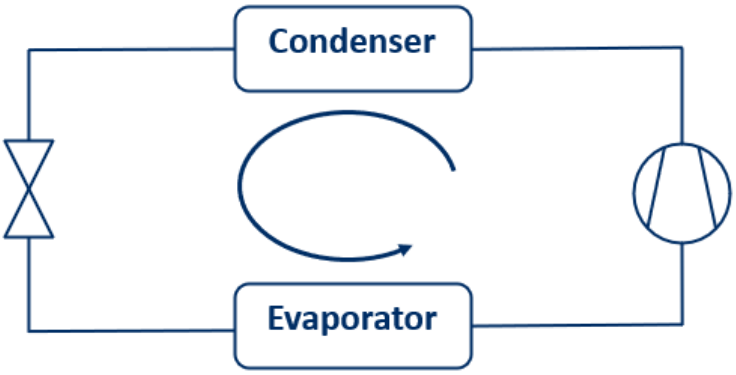

Figure 1.1: Schematic representation of a heat pump

The fluid starts in the evaporator, where it evaporates under low pressure, extracting heat from the surroundings. Next, the fluid is compressed in the compressor, increasing its pressure. Subsequently, the vapour phase condenses in the condenser, releasing heat to the surroundings. After, the fluid is expanded in the expansion valve to restart the cycle.
This process can be represented in a P-h diagram, as shown in Figure 1.2.

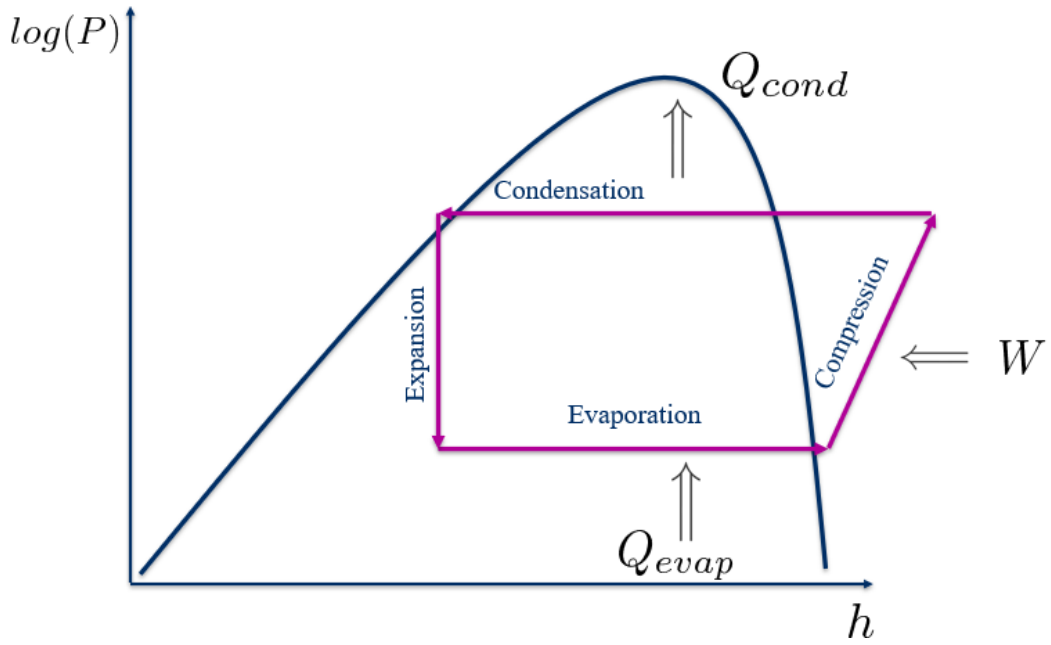

Figure 1.2: Pressure-enthalpy diagram of an ideal heat pump

After passing the expansion valve, the fluid expands. Consequently, some fluid evaporates due to a decrease in pressure. This causes a two-phase flow to enter the evaporator. Since the evaporator consists of several parallel tubes (in order to decrease the pressure drop across the evaporator), the liquid and vapour refrigerant need to be evenly distributed across these parallel tubes, which is performed by the manifold. The maldistribution of the two phases can cause a decrease in Coefficient of Performance (COP), and in some scenarios even ice formation on the outside of the evaporator [1]. Consequently, in order to be able to optimise future heat pumps, a good understanding of the phase distribution becomes crucial. The parameters influencing this maldistribution of the two phases are investigated in literature which include the channel diameter, channel orientation, etc. [2].

2 Objectives

The objective of this thesis is to investigate the phase distribution inside the manifold, which can be represented as an impacting T-junction. This investigation could be performed using measurements, but since these measurements require a significant amount of time and lack accuracy, a quasi steady state CFD model will be constructed.
This CFD model should be able to model the continuously changing interface between the different phases, which includes e.g bubble formation. However, due to this changing interface, describing two phase flow is relatively complex. As a result different CFD modelling approaches exist, all of which have certain advantages and disadvantages. For this reason these models need to be weighed against each other.
In order to be able to weigh these models against each other an investigation will be performed, which will be based on a literature survey. This literature survey will also include an investigation towards the different factors which may influence the phase distribution.

In order to check the accuracy of the model, testing is necessary. Afterwards, simulations will be executed. In this way, the influence of different inlet conditions and fluid properties on the phase distributions will be tested. After finishing these simulations, the results will be compared with measurements from the literature. Hence it becomes possible to explain the results of the simulations.

3 Two-phase flow

Two-phase flow occurs in many applications including nuclear power, chemical and space industries. For this reason over the last years an increasing interest in two-phase flow has arisen. However, due to the varying liquid-gas interface and the convective heat and mass transfer a significant amount of effort is still needed in order to fully understand or describe this phenomenon [3].

3.1 Fundamental quantities in two-phase flow

In order to facilitate the description of two phase flow, several commonly used quantities need to be distinguished.
The first quantity is the vapour quality. This vapour quality (x), which is defined in Eq.3.1, is the ratio of the vapour mass flow rate ($\dot{m}_g$) to the total mass flow rate ($\dot{m}_l + \dot{m}_g$).

$$x = \frac{\dot{m}_g}{\dot{m}_l + \dot{m}_g} \tag{3.1}$$

This vapour quality is often confused with the void fraction, which is defined as the area (of the cross section of the tube) occupied by the vapour phase in comparison to the total cross section of the tube.

$$\varepsilon = \frac{A_g}{A_l + A_g} \tag{3.2}$$

In the case of the velocity of a two phase flow in a tube, different definitions exist in the literature. According to Moreno [4], the two most commonly used velocity definitions are the superficial velocity and the true averaged velocity.
The true averaged velocity can be seen as the actual velocity at which the fluid passes through the tube. The average is determined by the volumetric flow rate of a certain phase through the area, occupied by that specific phase. Therefore, the true average liquid and vapour velocity is defined in Eq.3.3 and Eq.3.4, where the mass flux (G) is defined as $G = \frac{\dot{m}}{A}$.

$$u_g = \frac{\dot{V}_g}{A \times \varepsilon} = \frac{\dot{V}_g}{A_g} = \frac{G}{\rho_g}\frac{x}{\varepsilon} \tag{3.3}$$

$$u_l = \frac{\dot{V}_l}{A \times (1-\varepsilon)} = \frac{\dot{V}_l}{A_l} = \frac{G}{\rho_l}\frac{1-x}{1-\varepsilon} \tag{3.4}$$

The other way of defining the velocity of the two phases is by means of the superficial liquid and vapour velocity. These superficial velocities can be interpreted as the velocity a certain phase would have in absence of the other one. Thus, one defines these velocities as:

$$J_l = \frac{\dot{m}_l}{A \times \rho_l} = \frac{\dot{V}_l}{A} \tag{3.5}$$

$$J_g = \frac{\dot{m}_g}{A \times \rho_g} = \frac{\dot{V}_g}{A} \tag{3.6}$$

The superficial velocity describes the velocity of a phase by neglecting the presence of the other phase [5].

3.2 Forces in two-phase flow

In a two-phase flow, different forces, including the gravitational, inertia, viscous and pressure forces play a role on the phase separation [2]. By changing the flow conditions, including the (superficial) velocity of each phase, the void fraction, etc., the ratio between these different forces changes. In this way, changing the inlet conditions should change the phase separation. For this reason it becomes almost possible to separate the influence of the different parameters on the phase separation.
However, since all these parameters are all influenced by each other, a total separation of the influence of the different parameters is not possible.

In order to facilitate the description of the ratio between these different forces. Multiple characterising dimensionless numbers are defined in literature. The most important ones relating to two-phase flow are discussed in this section.

The first number, which is called the Reynolds number expresses the ratio between the inertia and the viscous forces. The Reynolds number is often used for determining if a flow is laminar or turbulent. The definition of the Reynolds number is given in Eq.3.7.

$$Re = \frac{\rho u L}{\mu} \tag{3.7}$$

Also a ratio for the gravitational and the inertia forces can be made. This is called the Froude number, which is defined in Eq.3.8, which is used for determining if a flow is sub- or supercritical.

$$Fr = \frac{u^2}{gL} \tag{3.8}$$

The Weber number defines the ratio between the inertia and surface tension forces. This number is often used for determining if a sharp boundary between a liquid and a vapour phase is present.

$$We = \frac{\rho u^2 D}{\sigma} \tag{3.9}$$

The surface tension can also be weighed against the viscous forces, which is called the Capillary number. The capillary number can be used to determine if bubble formation will occur.

$$Ca = \frac{\mu u}{\sigma} \tag{3.10}$$

The numbers, described above apply only for one phase. In cases featuring multiphase flow these quantities need to be averaged. This can be done by using the void fraction, except for the Weber and the Capillary number which need to be calculated for each phase separately.

3.3 Flow regimes

An important way to classify a gas-liquid flow is by flow regimes. These flow regimes describe the physical distribution of the two phases inside e.g. a pipe. The different regimes are listed on Figure 3.1.
According to Matovu et al.[6], different flow regimes exist for horizontal and for vertical oriented tubes.

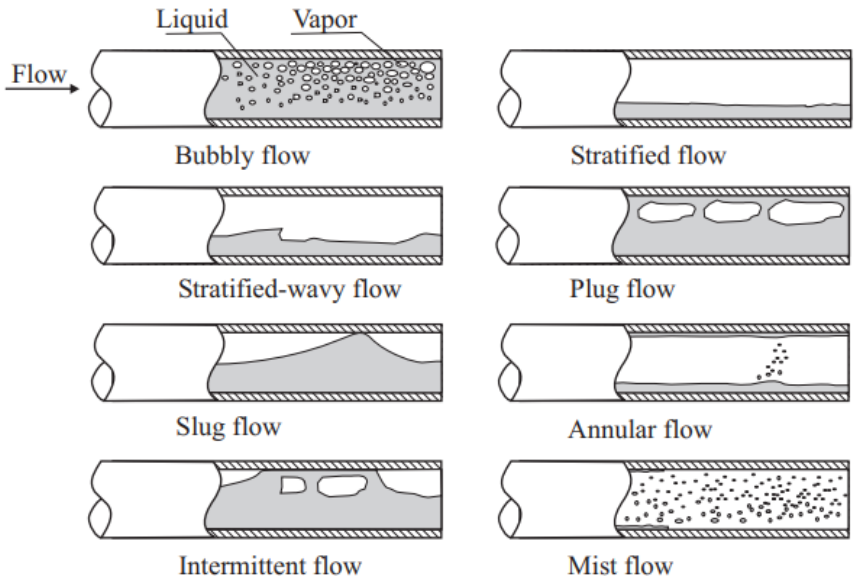

Figure 3.1: Visual representation of the different flow regimes for horizontal tubes [4]

Many other flow regimes, which are not displayed in Figure 3.1, are proposed in the literature. However, these omitted flow regimes occur when transitioning between the flow regimes presented in Figure 3.1.

3.3.1 Stratified (S) and Stratified wavy (SW) flow

Stratified flow is characterised by a complete separation between the different phases, where the liquid phase only exists at the bottom and the vapour phase only exist at the top of the tube. The complete separation is caused by the low values of the liquid and vapour superficial velocity [7]. Sometimes the interface between the two phases becomes wavy, then a stratified wavy flow pattern is obtained.

3.3.2 Plug flow (P)

By increasing the superficial liquid velocity, the smooth interface between the two phases disappears. In this way, long elongated bubbles are formed. These bubbles are small compared to the cross section of the tube [7].

3.3.3 Slug (SL) and Intermittent (I) flow

Unlike the plug flow, the diameter of the bubbles formed in a slug flow regime can become as large as the diameter of the tube.
This flow regime occurs for medium superficial vapour and for low superficial liquid velocities [5].
When the mass flux is increased even further, these slugs become larger. In this case an intermittent flow regime is obtained. This intermitted flow regime is characterised by large amplitude waves, which are altered by smaller waves.

3.3.4 Bubble flow (B)

By the bubbly flow regime, vapour bubbles are carried through the liquid phase. These bubbles are significantly small in comparison with the cross section of the tube and travel at a different velocity compared to the liquid phase.

3.3.5 Annular flow (A)

In some cases the vapour, which can contain small liquid bubbles, is surrounded by liquid. This is called the annular flow regime.
This flow regime only occurs for significant superficial vapour velocities.

3.3.6 Mist flow (M) and Dry-out (D)

In the case of mist flow, small liquid droplets are transported through a continuous vapour phase. This flow regime only appears for significant vapour qualities.
Dry-out is obtained when a transition between annular flow and a mist flow is made. In this case, small liquid droplets are dispersed in a continuous vapour phase, which is surrounded by a combination of a liquid film and dry areas on the tube walls.

3.4 Flow regime prediction

In order to predict the occurrence of a certain flow regime, various flow regime maps can be found in literature.
These maps predict the type of flow regime based on various quantities. Cheng [8] distinguishes two types of flow regime maps.
The first and most common type makes predictions based on the mass flux (G) and the vapour quality (x). Figure 3.2 provides an example of this type of flow map.

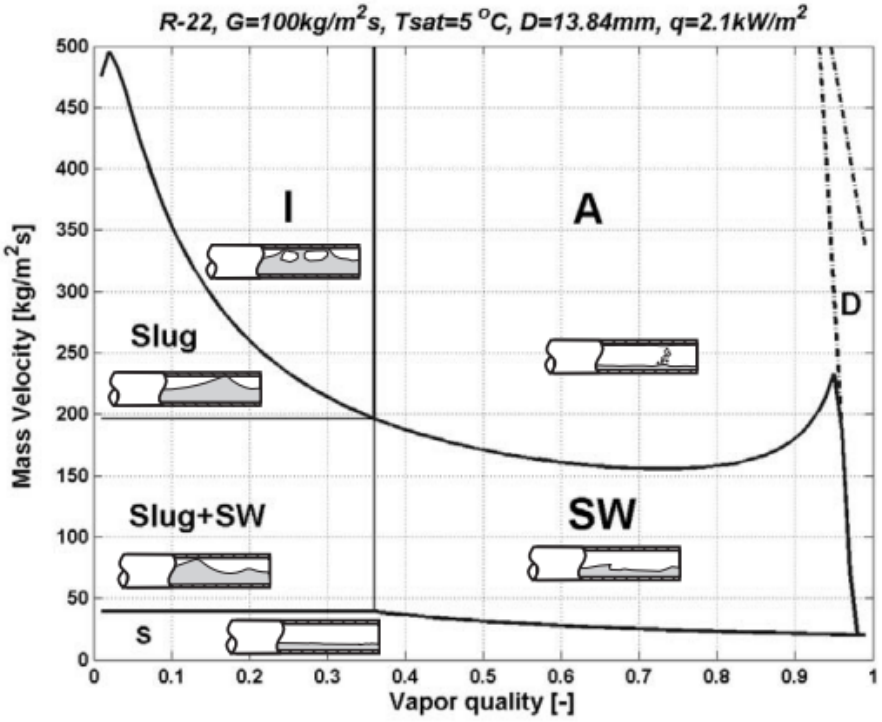

Figure 3.2: A flow regime map proposed by Moreno [4], for R32 with a saturation temperature of 5°C in a horizontal tube with an internal diameter of 13.84 mm

The second way to predict the occurrence of a certain flow regime is by means of the superficial liquid (x-axis) and vapour (y-axis) velocity. Which can be explained by using section 3.1, where it becomes clear that a combination of the mass velocity and vapour quality can be converted into a set of superficial velocities. Figure 3.3 provides an example of this type of flow regime map.
When dealing with CFD-simulations, this type of flow regime map may become more useful, in order to implement a certain flow regime. Due to the fact that these superficial velocities are easily converted to true averaged velocity.

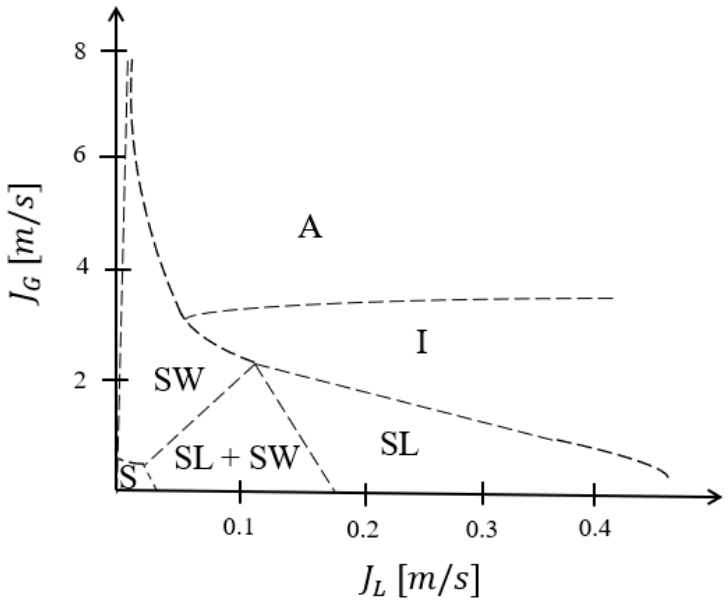

Figure 3.3: A flow regime map based on the superficial velocities for R32 at a saturation temperature of 10°C [9]

In section 3.2 the different forces acting on the phases were discussed and different dimensionless numbers were defined, such as the Weber number. Since the Weber number defines the ratio between the inertia and surface tension forces, it could also be used for creating a flow regime map, based on the liquid and vapour Weber number [10].

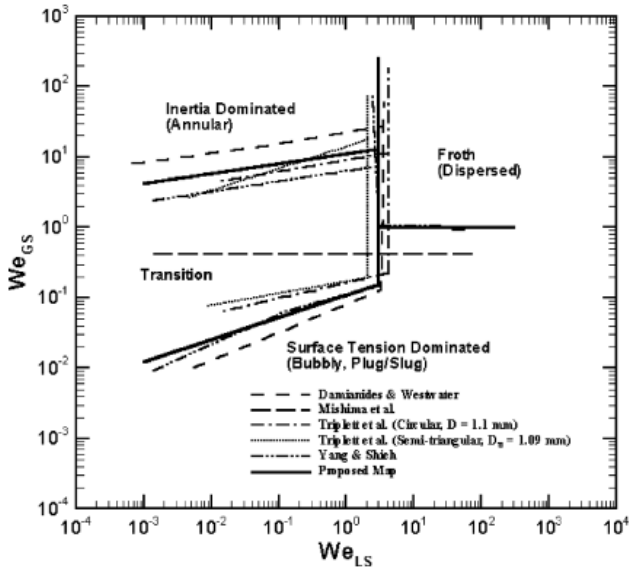

Figure 3.4: Flow regime map based on the Weber number [10]

It is very important to mention that the layout of a flow map depends on a variety of factors including the channel diameter, the channel orientation, the type of refrigerant, the channel geometry, etc. Consequently, these flow regime maps need to be determined experimentally each time a new refrigerant, channel diameter or channel orientation is used. During these experiments, the distinction between the different flow regimes is often based on visual examination. However, in reality the difference between different flow regimes is not always clear and are therefore influenced by a subjective opinion. Furthermore, as shown in Figure 3.2, typical flow regime maps contain a sharp interface between different flow regimes, implying an abrupt transition between different flow regimes. In order to overcome this subjectivity, Caniere et al. [11] proposes a more statistical way of representing the interface between the different flow regimes and therefore constructed a probabilistic flow regime map, which is shown on Figure 3.5

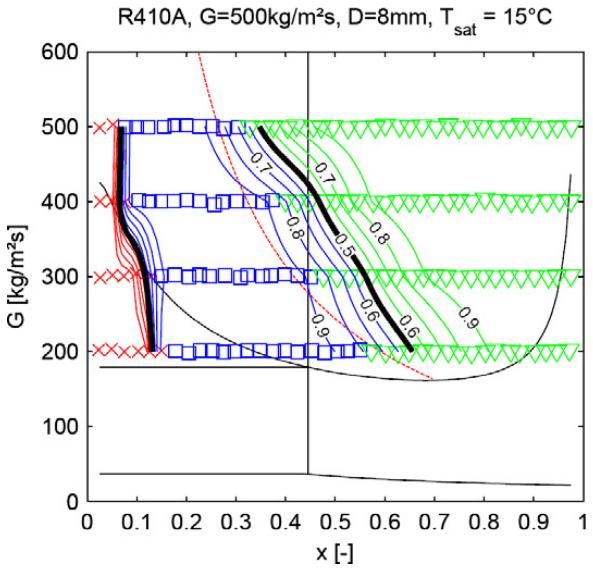

Figure 3.5: Probabilistic flow regime map for R410A in a channel with a diameter of 8mm [11]

3.5 Flow in a T-junction

T-junctions occur in different branches of industry, they are mostly used to distribute or to separate different phases. Two types can be distinguished. The first type is the branching T-junction, where the incoming stream does not perceive any direct collision with a wall of the junction. A schematic representation is shown in Figure 3.6.

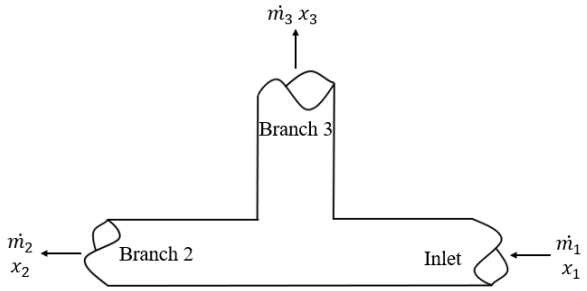

Figure 3.6: Schematic representation of a branching T-junction

The second type of T-junction that is frequently used is the impacting T-junction. This type of T-junction is displayed in Figure 3.7.
In contrast to a branching T-junction, an impact between the incoming flow and the wall of the junction does occur and, by turning one branch downwards, this T-junction can be used in some cases as a phase separator.
This thesis will deal with an impacting T-junction, with a horizontal inlet and vertical outlets.

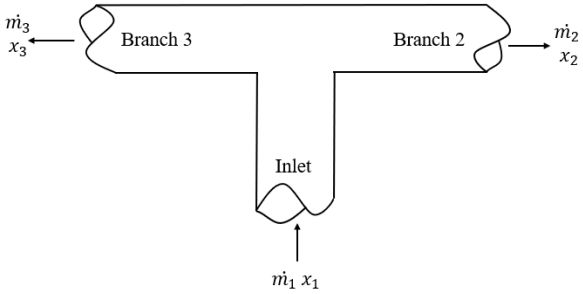

Figure 3.7: Schematic representation of a branching impacting T-junction

When conducting research into the phase distribution across the T-junction, it becomes necessary to define a new parameter that enables one to represent the resulting phase separation. For this reason, the liquid and vapour mass fraction are often defined as the fraction of the inlet liquid or vapour mass flow rate that goes into one outlet.

$$F_l = \frac{\dot{m}_{2,\mathrm{l}}}{\dot{m}_{1,\mathrm{l}}} \tag{3.11}$$

$$F_g = \frac{\dot{m}_{2,\mathrm{g}}}{\dot{m}_{1,\mathrm{g}}} \tag{3.12}$$

Using these parameters, F_l-F_g graphs, which provide insights into the distribution of mass fraction for a specific phase toward a particular outlet, can be constructed.
An example is shown in Figure 3.8.

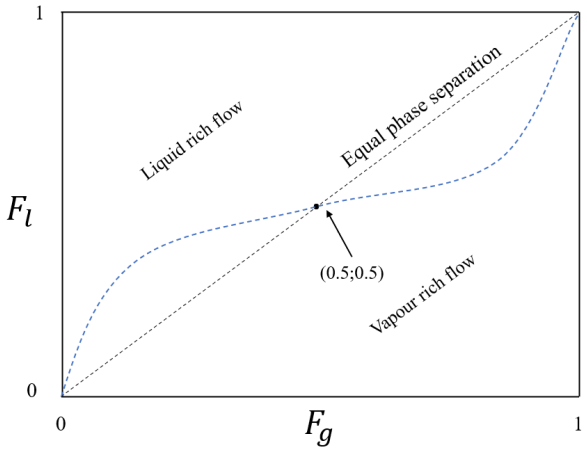

Figure 3.8: Example of an F_l-F_g flow map

The blue line indicates a possible phase separation scenario proposed by Billiet [5] on an impacting T-junction with horizontal branches. During this scenario, various measurements are conducted as the mass flow rate increases. The experiment begins at 0 mass flow rate towards the second branch, which is achieved by closing this second branch. Next, the experiment continues by opening the second outlet and varying the backpressure of one or both outlets, which results in an uneven distribution between the two branches. This is done until all the mass flows through the second branch and the third outlet is closed, which causes the mass fraction of the third branch to decrease from 1 until 0. According to the previously defined scenario, the blue line should start in the point (0;0) and it should end in the point (1;1).
In the case of a T-junction with horizontal branches no physical difference between the two branches can be perceived by the two phases and therefore the blue line has to cross the black point, where the liquid and vapour phase are split evenly across the two outlets [5].
By increasing the mass flow rate towards the second branch and hence moving along the blue line, two different areas can be distinguished. The first area is the area above the equal phase separation line, which is called the liquid rich flow area. The results located in this area, represent a liquid rich flow (at the second outlet), compared to a homogeneous flow. The same holds for the vapour rich area, where more vapour flows towards the second branch, compared to a homogeneous flow.

Since the phase separation does not only depends on the inlet mass flow rates, it is also possible to construct a chart similar to the chart of Figure 3.8 based on the void fractions and the mass fluxes. This type of map is used less in the literature and is therefore only mentioned for the sake of completeness.

3.6 Influence of different parameters on the phase distribution

The phase distribution across the T-junction is influenced by many forces, including gravitational, inertia, viscous and pressure forces [2]. These forces can be further categorised into line, surface and volume forces. By defining some characterizing numbers, these forces can be compared against each other, including the Reynolds number, which describes the ratio of the inertia and the viscous forces. Many other dimensionless numbers exist, including the Froude and Weber number. The most important ones were discussed in Section 3.2. The significance of each force is influenced by many factors. In order to be able to declare the results obtained in Section 8, a proper understanding of these influencing factors is crucial. Therefore in this section these influencing factors will be discussed extensively.

3.6.1 Influence of the channel diameter

Considering an increasing channel diameter while keeping the inlet velocity constant, the inertial forces increase as a result of the increasing mass flow rate. For this reason changing the internal diameter of the T-junction influences the relationship between the different forces and thus the internal diameter influences the split ratio of the two phases. For this reason, Sun et al. [12] investigated the influence of a changing outlet diameter on the phase distribution in an impacting T-junction for a nitrogen-water flow.
By comparing the phase separation results of different rectangular branch diameters for various flow regimes, the effect of a changing branch diameter on the phase separation of a slug flow was found to be small considering an increasing velocity [12].
Nevertheless it was found that for increasing branch diameters, the maldistribution of the two phases increases. This effect became negligible for considerable inlet velocities and was even less pronounced for annular flow. Mohamed et al. [13] investigated the validity of different analytical models proposed by Hwang et al. [14] and Ottens et al.[15], by using the same inlet velocities for different pressures and channel diameters. These models overestimated the influence of the channel diameter within the range tested by [13]. For this range (D = 13.5mm and D = 37.8mm), there was only a small influence of the channel diameter on the phase distribution. This finding was supported by Chen et al. [16], who investigated the influence of different inlet velocities for different channel sizes. Furthermore, it was found that the influence of the inlet velocity was decreased by decreasing the channel diameter. This was confirmed by Chen et al. [17], who observed no significant difference in phase split characteristics among micro-, mini-, and macro-sized impacting T-junctions. However, they also found out that for a decreasing channel diameter, the influence of the surface tension, which can not be overcome by the inertia forces (which are caused by the velocity) increases. In this way the slug bubbles did not break down. This causes these vapour slugs to flow into the branch with the greatest pressure gradient.
Despite the findings of Chen et al. [17], Ejaz et al. [18] states that geometry, which also includes the influence of the angle of inclination of the T-junction is the most influential factor to the phase distribution. This influence is caused by the ratio between the gravitational and inertial forces, which respectively depends on the mass flowrate and therefore also on the channel diameter. Additionally they also stated that by decreasing the diameter ratio the phase separation is increased.
However, as it became clear, these findings are not supported by the other references, which were unable to show a significant influence of the channel diameter on the phase distribution.

3.6.2 Influence of the superficial velocity

Since the superficial liquid and vapour velocities directly influence the significance of the inertial forces, these superficial velocities significantly impact the phase separation. For this reason, these velocities are investigated by multiple sources.
Billiet [5] stated that for higher superficial liquid velocities, the liquid is more dispersed as droplets. For an increasing superficial vapour velocity, the droplet size increases. As these small droplets are transported more easily, the fluid is more likely to flow in both channels. In this way the phase maldistribution is decreased.

Since the slug length is influenced by the superficial liquid velocity, Chen et al. [17] found out that the inlet vapour superficial velocity has a smaller influence on the split ratio in comparison to the liquid superficial velocity, which can be attributed to the fact that longer slug bubbles are more likely to break up in comparison to smaller bubbles and the fact that smaller bubbles are transported more easily towards the branch with the greatest pressure gradient.

El-Shaboury et al. [19] investigated the influence of the superficial velocity for a stratified wavy and an annular flow regime in a horizontal impacting T-junction for an air-water flow. It was found that for an increasing superficial liquid or vapour velocity the maldistribution of both flow regimes increased.
Elazhary et al. [20] conducted research into the influence of the superficial velocities on the phase separation of an impacting T-junction with a rectangular cross section for an air-water mixture. The same results as found by El-Shaboury et al. [19] were observed. However due to the small size of the junction, the influence of a changing superficial velocity was less pronounced compared to bigger junctions.

Memon et al [21], also conducted research to the influence of the superficial velocity on the phase separation for branching T-junctions. This was done by varying the superficial vapour velocity for a constant superficial liquid velocity and vice versa. By increasing the superficial vapour velocity the liquid carry-over into the side arm (= the thirth branch on figure 3.6) increased. Contrary, by increasing the superficial liquid velocity, the liquid carry-over was decreased, due to the increase of the mass flow rate which results in a higher influence of the inertial forces.
When both superficial velocities were increased simultaneously, no significant effects were observed until a certain ”gas threshold value”, which depends on the superficial velocities, was reached. Below this gas threshold value, only vapour was carried into the side arm. Beyond the gas threshold value, liquid was also carried into the side arm.
In summary, it can be stated that the influence of the superficial vapour and liquid velocity depends on the type of T-junction. However, for impacting T-junctions multiple sources agreed on the positive effect of the superficial velocity on the phase distribution. In this way it was found that increasing either the superficial vapour or liquid velocity resulted in a more even distribution of the phases.

3.6.3 Influence of the orientation of the T-junction

When the density difference between vapour and liquid refrigerant is considered to be significant the influence of the gravitational force differs for the vapour and liquid phase. It is for this reason that a change in orientation of the T-junction influences the phase separation. Based on this reasoning, for a horizontal T-junction with vertical outlets, the influence of the gravitational force (which depends on the orientation of the junction) should be maximal.
Considering the orientation of the gravitational forces, one defines the angle of inclination as the angular difference between a horizontal impacting T-junction with horizontal branches and an impacting T-junction with vertical branches.
Figure 3.9 provides a schematic representation of the angle of inclination.

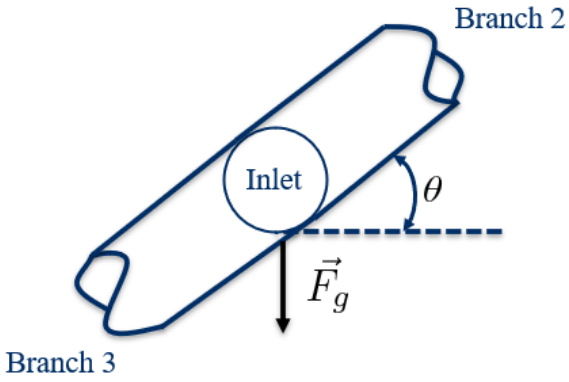

Figure 3.9: Schematic representation of the angle of inclination

Mohamed et al. [22] investigated the influence of the angle of inclination on the phase separation. They found that the degree of maldistribution of a certain angle of inclination depends on the inlet conditions. However, the tendency for a greater maldistribution became worse for an increasing angle of inclination. They also found that this maldistribution became even worse when a stratified flow regime was present.
These findings were confirmed by Mohamed et al. [23], who futhermore found out that at low speeds, for any angle of inclination, full separation between the different phases was obtained. For this reason, they investigated three scenarios.
In the first scenario, the angle of inclination was maintained below 30°. During these experiments, no liquid came out of the second outlet. However, in the second branch standing wave of the liquid phase was detected. The size of this standing wave depended on the angle of inclination and the superficial velocities.
The second scenario, included angles between 60° and 90° with a superficial liquid velocity below 0.8 m/s. Initially no liquid was carried over into the second branche. As the superficial liquid velocity was increased beyond a sudden Jl-value, liquid was carried into the second branch.
For the last scenario, the same angles of inclination as the second scenario were used. However this time, the superficial vapour velocity was kept below 3 m/s. When the superficial liquid velocity was increased beyond a certain value, liquid was flowing out of the second branch.

Considering the sources mentioned in this section, the influence of the angle of inclination is found to be significant as increasing this angle of inclination results in a greater maldistribution. However, increasing the superficial velocity results in a decreasing maldistribution.

3.6.4 Influence of the fluid properties

Since the phase separation is influenced by gravitational, viscous and inertial forces, it can be expected that different refrigerants with different fluid properties, including density and viscosity should have different phase distributions [2]. By applying the previously mentioned trends to an impacting T-junction with a horizontal inlet and vertical outlets where a refrigerant with considerable liquid density and a low vapour density flows. The phase distribution is expected to be non-uniform, due to the gravitational forces. Nevertheless for fluids with notable surface tensions, the flow is likely to form bubbles after impact with the vertical wall of the junction. According to Billiet [5], bubbles are transported easily to the upper outlet and as the droplet size decreases, the droplets are transported more easily in the opposite direction of the gravity vector.
Billiet [5] notes that the literature on the influence of the fluid properties on the phase separation is rather limited. However, Chen et al. [17] conducted an investigation on the influence of surface tension and found that for a decreasing surface tension a more even phase distribution was achieved. As for a decreasing surface tension, the bubbles formed during the collision become smaller and are thus transported more easily. However, it was also found that for an increasing superficial vapour velocity, the influence of the surface tension decreases.
Based on [5], [2] and [17], it can be stated that the influence of the fluid properties on the phase distribution can be brought down to the influence of the surface tension and the density.

3.6.5 Influence of the pressure

The total pressure is found to be an important parameter, influencing the phase separation. For two-phase flow the total pressure drop is caused by the pressure drop due to friction, acceleration and a difference in height [8]. Taking these factors into account, one obtains Eq.3.13.

$$\frac{dP_{\text{total}}}{dL} = \frac{dP_{\text{friction}}}{dL} + \frac{dP_{acceleration}}{dL} + \frac{dP_{height}}{dL} \tag{3.13}$$

According to Balasubramaniam et al. [24], the total pressure drop in a two phase flow is mostly caused by friction, more precisely the friction caused by the wall. This friction term can be described by Eq.3.14 [24].

$$dP_{\text{friction}} = (1 + CX + X^2)dP^* \tag{3.14}$$

Where the coefficient (C) needs to be determined experimentally, P* represents the internal pressure in the liquid phase, and X (also called the Lockhart-Martinelli parameter) represents the two-phase pressure gradient, which is defined as:

$$X = \frac{\sqrt{dP_{\text{liquid}}}}{\sqrt{dP_{\text{vapour}}}} \tag{3.15}$$

The pressure influences the occurring flow regime, due to the fact that the bubble breakdown of e.g. a bubbly flow is caused by pressure forces which are the result of turbulence [20].

The literature on the pressure drop in an impacting T-junction is limited. However Das et al. [25] investigated the influence of the pressure on the phase split by testing different superficial velocities for different pressures. In this way, they found a decreasing influence of the pressure on the phase separation for a decreasing superficial vapour velocity.
Azzi et al. [26] also investigated the influence of the pressure on the phase distribution in a branching T-junction using a pressure of 0.13 and 0.18 MPa for a liquid superficial velocity of 0.41 m/s and a vapour superficial velocity of 2.35 m/s. It was found that for higher pressures, the maldistribution becomes slightly worse.

Mohamed et al. [13] investigated the influence of the pressure on the phase separation which was found to depend on many factors, including the pipe diameter, orientations, etc. They also stated that at the moment of publishing (the paper was published in 2018) no exact correlation between pressure drop and phase separation has been found.
Nevertheless, multiple sources, including [5] and [13] conducted research into a mathematical description of the pressure drop across an impacting T-junction. However for impacting T-junctions no significant research towards the influence of the pressure on the phase distribution has been conducted.

4 CFD modelling of two-phase flow

Modelling two-phase flow is a complex task due to the continuously changing interface between the two phases. To address this complexity, different modelling approaches have been developed, including reduced order models, empirical correlations and CFD modeling. In the case of reduced order models, different types exist, including the drift flux, the separated flow and algebraic slip model.
In this thesis the modelling will be done using CFD simulations as this approach enables identifying and investigating the effect of certain physical parameters in order to be able to obtain a thorough understanding of the phase distribution in an impacting T-junction.

The CFD modelling technique for two phase flow can be subdivided into two main approaches. The first approach is the Euler-Euler approach, which models the fluid as a continuous medium and can be subdivided into various techniques such as Mixture and Eulerian modelling and the Volume of Fluid (VOF) method. The second approach is the Euler-Lagrange approach.

These two approaches, along with the specific modelling techniques mentioned above, are illustrated in Figure 4.1.

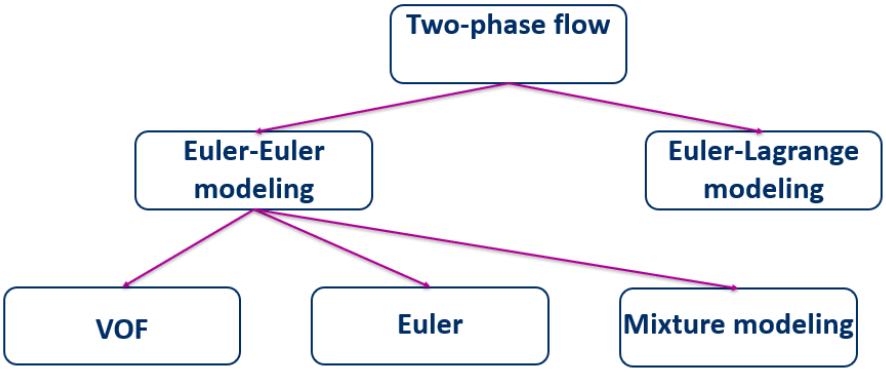

Figure 4.1: Different modelling techniques for two-phase flow

This chapter will discuss these different approaches and their mathematical fundamentals which will also include some typical use cases.

4.1 Euler-Euler approach

For modelling multiphase flow, multiple options are available. One possible approach is to mathematically treat each phase individually [27], also known as the Euler-Euler approach.
The Euler-Euler approach is further subdivided into different categories, including: Mixture modelling, Eulerian modelling and the volume of fluid method (VOF).
In each approach the conservation equations are solved for each phase separately. These conservation equations consist of the conservation of mass (also called the continuity equation), which is displayed in Eq.4.1, the conservation of momentum (Eq.4.2) and in some cases also the conservation of energy.

$$\frac{\partial \rho}{\partial t} + (\nabla \rho \mathbf{u}) = 0 \tag{4.1}$$

$$\rho \frac{\partial \mathbf{u}}{\partial t} + \nabla(\rho \mathbf{u} \cdot \mathbf{u}) = -\nabla p + \mu \nabla^2 \mathbf{u} + \rho \mathbf{g} + \mathbf{F}_{\text{surface tension}} \tag{4.2}$$

For incompressible fluids the continuity equation simplifies to Eq.4.3.

$$\nabla \mathbf{u} = 0 \tag{4.3}$$

4.1.1 Mixture models

In the case of the mixture model, the multiple phases are treated to be one homogeneous phase. Consequently, only one set of conservation equations needs to be solved. These equations use averaged quantities, including the averaged density and averaged viscosity. For this reason, this type of modelling is considered to be the most simple one.
In order to justify the usage of a mixture model, Silva et al. [28] states that some conditions need to be fulfilled.

- A local equilibrium between the different phases need to be established
- The density of each phase needs to be more or less constant
- Both phases have to share the same velocity field

In this thesis many inlet conditions are tested, with some featuring significant vapour qualities. This causes phase instability and a lack of local equilibrium, therefore the homogenous mixture approach will be inappropriate for the cases being studied in this thesis. For this reason these mixture models will not be used in this thesis and are only mentioned for the sake of completeness.
For more detailed information about mixture models, the reader is referred to [28].

4.1.2 Eulerian models

Eulerian models model each phase separately. Therefore the conservation of momentum and mass are solved for each phase separately, which increases the computational time. Eulerian models also contain some other limitations, including the inability for solving inviscid flows [29]. In order to be able to solve the conservation equations coupling between the different phases is needed, which is achieved by the usage of interphase exchange coefficients and closure equations, which are based on empirical results or are derived mathematically. These correlations provide information about the interphase momentum transfer, which states that the momentum transfer of the vapour phase on the liquid phase equals the momentum transfer of the liquid phase on the vapour phase.
The momentum transfer is determined by the drag, virtual mass, lift and turbulent dispersion force [30].

$$\overline{M_l} = \overline{M_g} = F_D + F_{VM} + F_L + F_{TD} \tag{4.4}$$

Eulerian modelling is used for immiscible flows where small particles or bubbles flow through a continuous phase. Thus, Eulerian modelling is only used for simulating small vapour qualities, which is not the case in this thesis.

4.1.3 VOF modelling

The VOF method is used for cases in which the interface between the different phases needs to be captured.
In this way, the VOF modelling technique is able to model large bubbles. Due to these properties, the VOF modelling technique was used for constructing the model of Section 6.

During the VOF modelling approach, the two phases are considered to be non-interpenetrating as this would result in a more "blurry" interface between the different phases [31].
In order to be able to carefully capture the interface between the different phases, VOF captures the volume fraction of each cell. This is done by solving an extra transport equation, which captures advection.
In this thesis the VOF approach is used to only solve the conservation of mass and momentum and hence the conservation of energy is neglected. These conservation equations are only solved once for each mesh cell which creates the need of defining different mixture parameters. Therefore one defines the mixture density and viscosity as:

$$\rho = x\rho_{\text{vapour}} + (1-x)\rho_{\text{liquid}} \tag{4.5}$$

$$\mu = x\mu_{\text{vapour}} + (1-x)\mu_{\text{liquid}} \tag{4.6}$$

The volume fraction ($0 \leq H \leq 1$) is calculated by using the following transport equation [32], where $H(\mathbf{x},t)$ represents the volume fraction. When the volume fraction is averaged over each cell, then this is denoted as $\overline{H}(\mathbf{x},t)$.

$$\frac{\partial H}{\partial t} + \nabla(uH) = 0 \tag{4.7}$$

Eq.4.7 states that the change of the volume fraction of a cell is only caused by the velocity field of the two phases.

The volume fraction is needed for calculating the surface tension force, used in Eq.4.2, which can be calculated by Eq.4.8 [33].

$$F_{\text{surface tension}} = \sigma \kappa \nabla H \tag{4.8}$$

κ denotates the surface curvature between the different phases and can be calculated, using the normal vector to the interface between the different phases.

$$\kappa = -\nabla n \tag{4.9}$$

with

$$n = \frac{\nabla H}{|\nabla H| + \delta'} \tag{4.10}$$

Where δ' represents a small non-zero term in order to avoid the denominator to become zero [33].

Another approach for capturing interfaces between different phases is through the use of a level set method which represents the interface as the zero level set of a signed-distance function $(\phi(x,t))$, where:

$$\phi = \begin{cases} > 0 & \text{in one fluid phase,} \\ < 0 & \text{in the other fluid phase,} \\ 0 & \text{at the interface.} \end{cases} \tag{4.11}$$

This function is updated every time step using the following transport equation:

$$\frac{\partial \phi}{\partial t} + \mathbf{u} \cdot \mathbf{n} |\nabla(\phi)| = 0 \tag{4.12}$$

Where n denotates the normal vector of the interface between the different phases (Eq.4.10), which can be computed easily considering the often smooth value of the ϕ field [32].
After updating this function, it loses its signed distance property and therefore needs to be reinitialized, which can be done by recalculating the interface and the distance of every grid point to this interface. However, this method requires a lot of computational power and hence other methods are proposed in the literature. Many of these methods including the method proposed by Sussman et al. [34], which solves Eq.4.13, have problems considering the conservation of mass. For this reason, different "conservative level-set methods" are also proposed in the literature.

$$\phi_\tau = sgn(\phi^0)(|\nabla \phi| - 1) \tag{4.13}$$

sgn denotates a smoothed signum function.

For more information about level-set methods, the reader is referred to [32].

4.2 Euler-Lagrange approach

The Euler-Lagrange approach models one continuous phase, containing another non-continuous phase. For this reason, the Euler-Lagrange approach is used for simulating small particles or even solid objects which are transported through a vapour or liquid phase. These particles or solid objects are small compared to the smallest turbulence length scale [35]. In this way, the continuous phase is treated as the Eulerian phase where equations 4.1 and 4.2 are solved. For the non-continuous phase the equations of motion are solved. This enables tracking the streamline of the dispersed particles. However, according to Persson [36], the Euler-Lagrange approach encounters some limitations. Including a high computational cost for simulating significant amount of particles (which are assumed to be spherical) and the inability to solve for dispersed phases with a volume fraction, greater than 10%.

$$\frac{dx_i}{dt} = \vec{u}_i \tag{4.14}$$

$$\sum \vec{F}_i = m_i \frac{d\vec{u}_i}{dt} \tag{4.15}$$

Where $\vec{x}_i$, $\vec{u}_i$ and $\vec{F}$ are the particle position, the particle velocity and the external forces. These external forces include gravitational forces, buoyancy forces, drag forces, pressure forces, etc.

4.3 Turbulence modelling

In the case of a two-phase flow, turbulence often occurs. Modelling this turbulence can be done, by three different approaches.
The first approach is to not use a turbulence model in combination with a 'fine' grid and a small time step. This approach results in precise modelling of the occurring turbulences. However, due to the small grid size combined with the small time step, it requires a significant amount of computational time.
A second approach for modelling turbulence is by including a turbulence model. For this manner many turbulence models have been developed, all of which seek to find a mathematical closure for the Reynolds averaged Navier-Stokes equations, which include some nonlinear terms. In this way different models exist in the literature, including the k-ε-model and the k-ω-model. For more information on these turbulence models and their mathematical background, the reader is referred to [37].
By, including a turbulence model, the amount of mesh cells can be minimized, which results in minimal computational time. However, as these turbulence models often require the input of one or more experimental or mathematical determined constants, they were not used in this thesis.
A last possible approach to model turbulence is by using a combination of the two previously mentioned approaches. In this way, in some places in the simulation the flow is assumed to be laminar, while in other regions a turbulence model is included.

5 Existing models

Different models, proposed by [14], [38], [39], [40], [41], [42], [15], and [19], for the prediction of the phase separation in an impacting or branching T-junction, exist in the literature. These models are summarised in Table 5.1.

Author	Mixture	Input	Output
Azzopardi et al. [38]	water-air	F_l	F_g
Azzopardi et al. [39]	water-air	F_g, E, orientation	F_l
Chien and Rubel [40]	water-steam	F_g, x_1	F_l
Hong and Christon [42]	water-steam	$\dot{m}_1$, x_1, D, F_g, fluid properties	F_l
Ottens et al. [15]	water-air	J_l, J_g, D, F_g, fluid properties	F_l
El-Shaboury [19]	water-air	$\dot{m}_1$, x_1, $\dot{m}_3$, D, fluid properties, flow regime	F_l, F_g

Table 5.1: Summary of existing models for predicting phase distribution in T-junctions by Billiet [5]

The model of Ottens et al. [15] is derived from the mechanical energy balance, where the energy loss of the junction is considered by using an "energy loss coefficient", which must be determined experimentally. This highlights the importance of accurately determining the value of this energy loss coefficient. Unlike the model of Ottens et al. [15] the model of El-Shaboury [19], started from the basic conservation equations for the two phases and is therefore considered to be more reliable [5].

Almost all of these failed to output acceptable results for the fluids and flow regimes, which were not used during the experiments for the development of the proposed model. Consequently, Billiet [5] proposed a new model for macro-sized impacting T-junctions which incorporates different constants which were obtained through various experiments where the pressure drop across the T-junction was calculated for different refrigerants.
This model was derived from fundamental laws, concerning the conservation of mass, momentum and energy. During development, certain terms in these conservation equations were neglected based on certain assumptions including, the absence of friction due to the small size of the control volume.
In this way, a flowchart which outlines an iterative process used for calculating $\dot{m}_3$, x_2, x_3 was constructed. This model was tested with multiple refrigerants, including R134a, R32, R1234ze, and R125, yielding reasonable results for almost every flow regime, except for the stratified-wavy flow regime. These less accurate results could be attributed to the limited number of tests that were performed for this flow regime. However, when the model was tested for an air-water and an water-steam flow, the results were still reasonable, but were worse compared to those obtained for the refrigerants. The reason for this could be the value of the model coefficients which were determined using data from experiments featuring various refrigerants but not water, air or steam mixtures.

The most recent analytical model found in the literature proposes a model developed for the prediction of the phase distribution in a vertical header with more than 30 branches [43]. These branches are a combination of different series connected branching T-junctions.
This way a flowchart is suggested by which the phase separation of each outlet could be predicted. The flowchart was tested using R410A. This model distinguishes itself from other models by also taking the liquid film thickness and intrusion depth of the branch pipes into account, as these two parameters have been shown to influence the phase distribution.

Few CFD models on phase separation inside a T-junction have been proposed in the literature. However, most of these models, including those by of Lu et al. [44] and Tran et al. [45], are not capable of modelling different flow regimes and bubble formation effectively.
Lu et al. [44] constructed a 3D CFD model of a branching T-junction using the Euler-Euler approach in combination with the k-ε turbulence model. They investigated the influence of multiple inlet parameters on the phase separation.
Tran et al. [45] also developed a 3D CFD model to investigate liquid carry-over in branching T-junctions for an air-water mixture. This study was conducted by altering the diameter ratios of the junction and using different superficial velocities.
The model produced reasonable results. However, the authors stated that a more detailed investigation into the phase distribution would require a model which uses the Volume of Fluid (VOF) approach.

6 The developed model

This thesis aims to investigate the influence of different inlet conditions on the phase distribution in a symmetrical impacting T-junction, with a tube diameter of 8mm. This is accomplished by building a two-dimensional Computational Fluid Dynamics (CFD) model. As it is impossible to capture the physics of a stratified flow regime in a two-dimensional horizontal T-junction with horizontal outlets, a model of a horizontal impacting T-junction with vertical branches is constructed.

For the development of the adiabatic model, which was built using a VOF approach in order to ensure a sharp interface between the different phases, the software StarCCM+ was used. The densities which were used were obtained from liquid and vapour tables for R410A.
In order to ensure a fully developed flow regime, the inlet length is chosen to be 55mm. However the branch length sizes 25mm, in order to ensure minimal vortices (which are caused by the impact with the wall of the junction) at the outlets.
This, combined with a fine grid to accurately capture the physics, results in a significant amount of grid cells. As a result, to ensure both optimal results and a minimal of computational time, performing a grid study becomes unavoidable. In this way a grid convergence study, following Roach's methodology [46] was used, resulting in triangular mesh with a grid size of 8.10^{-5}m.

Grid size	Average Vapour Mass Flow Rate at Upper Outlet $[\frac{kg}{m^2 s}]$
$1.0E-4\ m$	0.04638
$8.0E-5\ m$	0.04607
$6.0E-5\ m$	0.04268

Table 6.1: Example of Results from the grid convergence Study

Additionally, a Courant-Friedrichs-Lewy (CFL) number of 0.5 is chosen to determine the time step size for each iteration. This CFL describes the amount of cells crossed by the fluids during one time step. If this number exceeds 1, multiple cells are crossed during one time step, causing instability or inaccuracies.
The Courant number is therefore defined as:

$$CFL = \frac{u_{max}\Delta t}{\Delta x} \tag{6.1}$$

Where Δt and Δx respectively indicate the time step and the minimal mesh size.
As the influence of different vapour qualities and mass flow rates was investigated, a different time step was used for each simulation, calculated using Eq.6.2.

$$\Delta t = \frac{0.5 \times 8.10^{-5}}{u_{max}} \tag{6.2}$$

Figure 6.1 visualises the matter, discussed in this section.

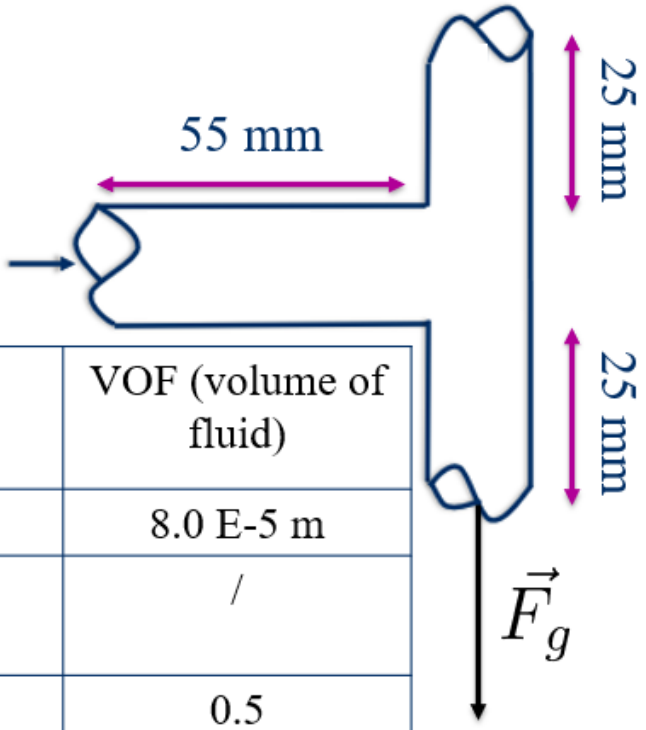

Modeltype	VOF (volume of fluid)
Mesh-size	8.0 E-5 m
Turbulence model	/
Courant number	0.5
Refrigerant	R410A

Figure 6.1: The developed model and its specifications

7 Simulations

In this thesis, multiple simulations, featuring R410A will be performed in order to investigate the influence of the mass flow rate and the vapour quality. Based on these parameters, the inlet conditions for the CFD simulation can be calculated by using a flowchart developed for this purpose.
All simulations in this thesis are conducted for a T-junction with a horizontal inlet and vertical branches.

7.1 Procedure

In order to be able to investigate the influence of the mass flux and the void fraction for R410A a flowchart was developed. This flowchart is displayed in figure 7.1.

First, the determination of a G- and an x-value is required. Based on these values, the superficial liquid and vapour velocities, which are necessary for calculating the void fraction, can be calculated. Next, the void fraction needs to be calculated which is essential in order to determine the inlet conditions for the CFD simulation. This void fraction can be calculated based on Eq.7.1 and Eq.7.2 [47].

$$\varepsilon = 1 - \exp\left[-1 - 0.3 \times ln(Ft) - 0.0328 \times (ln(Ft))^2\right] \tag{7.1}$$

With Ft:

$$Ft = \left[\frac{x^3 G^2}{\rho_g^2 g D(1-x)}\right]^{1/2} \tag{7.2}$$

These equations are based on data of R410A and R134a, flowing through a tube with an internal diameter of 7.04mm.

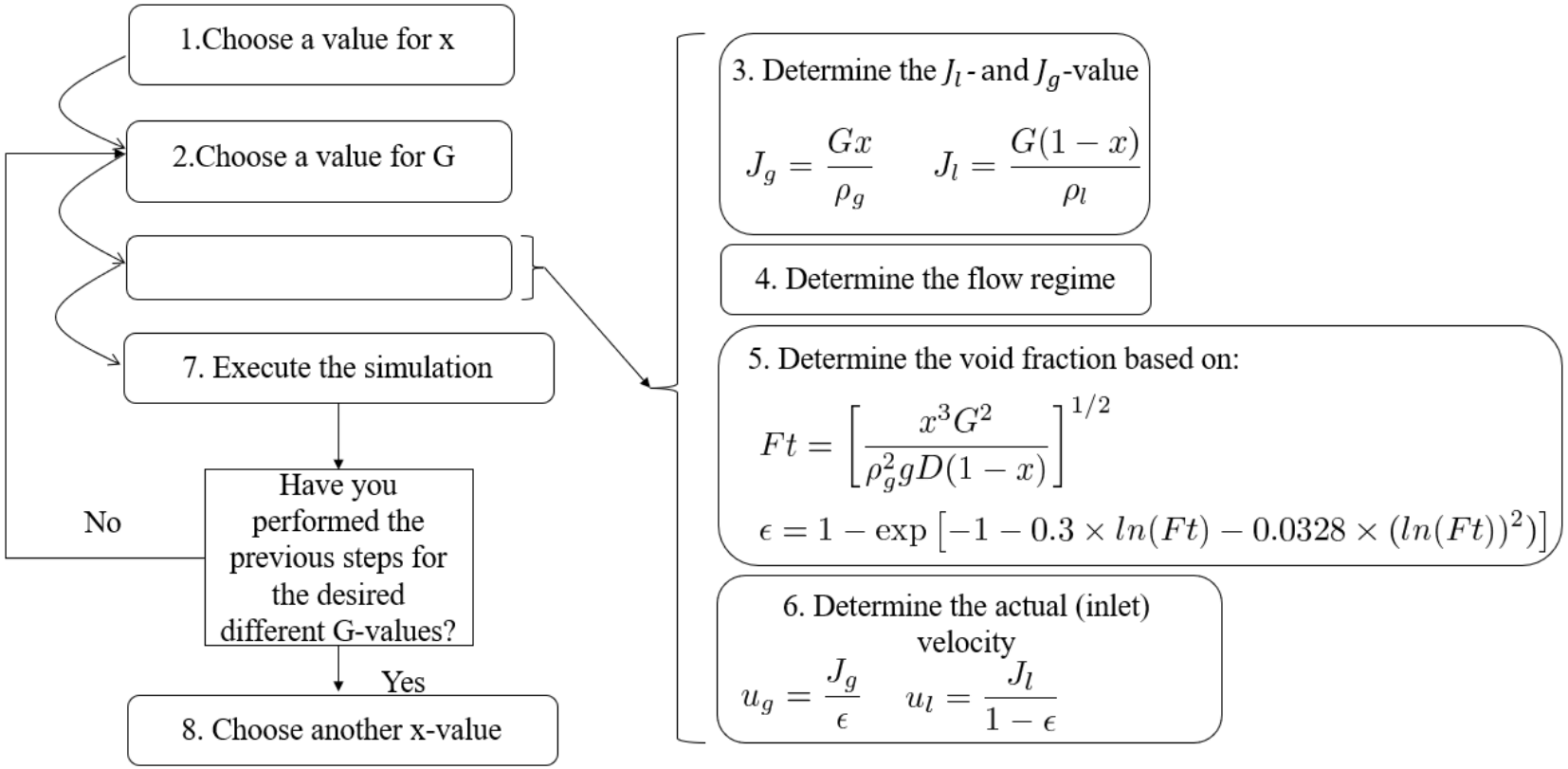

Figure 7.1: Flowchart of the simulation procedure used in this thesis

Determining the inlet conditions also involves knowing the occurring flow regime, which is possible by using the flow regime map presented in Figure 7.2, which is based on experiments executed for R410A inside a tube with an internal diameter of 8mm [48]. The saturation temperature during the experiments was chosen to be 10°C, which is the same as the saturation temperature chosen for the refrigerant used in this thesis (R410A).
The occurring pressure is determined in advance based on a fluid property table of R410A.
Figure 7.2 shows the used flow regime map on which the G- and x-values of the simulations performed in this thesis are plotted.

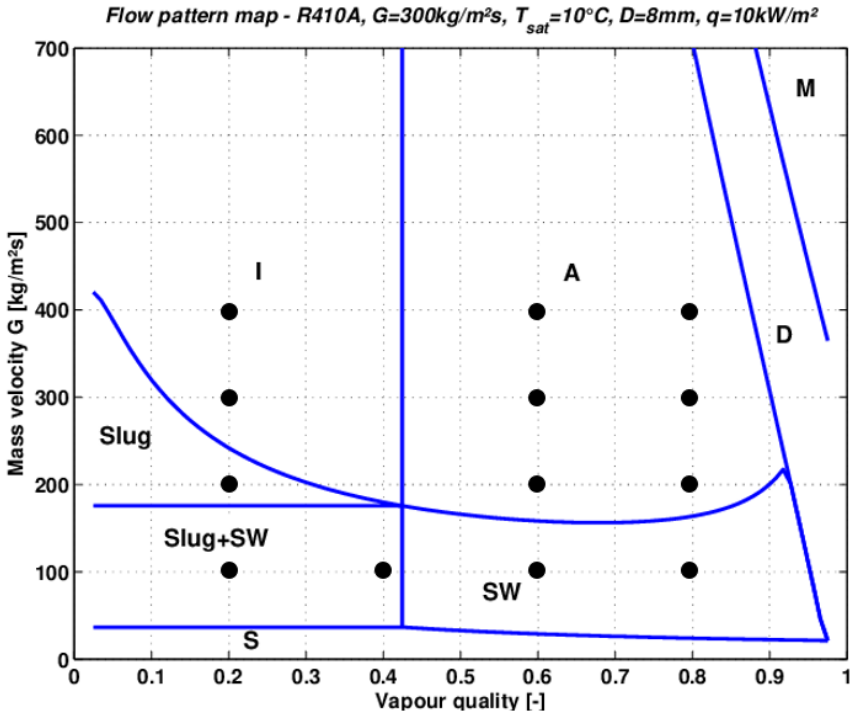

Figure 7.2: Flow regime map for R410A at 10°C saturation temperature in an 8mm diameter tube, depicting the values simulated in this thesis [48]

Figure 7.2 makes clear that different flow regimes will be tested multiple times. In this way it also becomes possible to compare the results of different flow regimes.
However, mist and dry-out flow will not be investigated as a different modelling approach is necessary to model these flow regimes.

After choosing an x- and G-value the next step is to determine the actual inlet velocity, which can be done based on the Eq.7.1 and Eq.7.2.
After performing the simulation, repeating the previous steps for different mass fluxes maintaining the same x-value, enables the influence of the mass flux to be investigated. After this, all these steps can be repeated for different x-values and hence exploring the influence of both the vapour quality and the mass flow rate becomes possible.
Figure 7.1 illustrates the sequential steps outlined in this section.

8 Results

During this thesis, multiple simulations were performed using the model developed in Section 6. Through these simulations, the influence of different parameters on phase separation was investigated. The results described in this chapter are based on measurements of the mass flow rates of each phase from the second branch, which was directed downwards.

8.1 Mass flux

By comparing the results of a constant vapour quality, featuring different mass fluxes, Figure 8.1 is obtained. The plot displays results for annular flow regimes with a vapour quality of 0.6 and various mass fluxes in an Fl-Fg graph.
In this way an analysis was conducted towards different mass fluxes, simulated for a constant x-value, except for G = 100 $\frac{kg}{m^2 s}$, which resulted in a stratified wavy flow regime instead of an annular flow regime, as shown in Figure 7.2.
It becomes clear that by increasing the mass flux, the phases are distributed more evenly, as the points in Figure 8.1 converge towards [0.5;0.5], where both phases are evenly distributed.
Additionally, it is observed that for each simulation, the vapour phase is distributed relatively evenly. However, due to the gravitational force in combination with the orientation of the junction, most of the liquid is pulled downwards, in the direction of the gravitational vector.

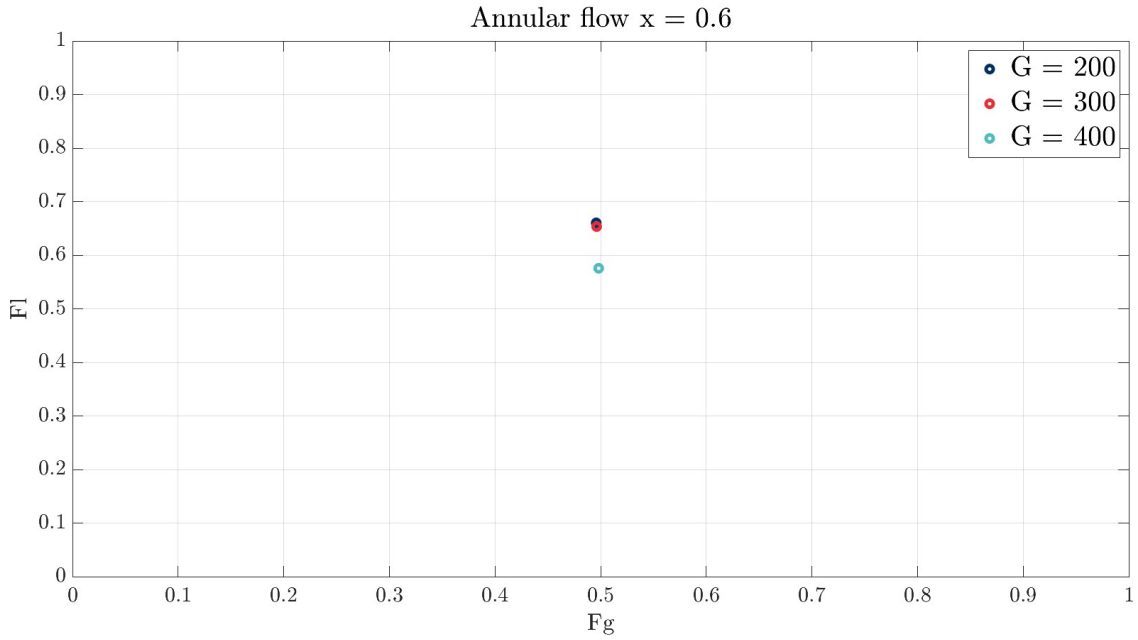

Figure 8.1: Results for annular flows featuring different mass fluxes, with a constant vapour quality of 0.6

The same plot (also for the results of the second outlet) was created for annular flow regimes featuring a vapour quality of 0.8. These results are displayed in Figure 8.2, where the same trends as in Figure 8.1 are present, indicating a decreasing preference of the liquid phase to flow downwards as the mass flux increases. However compared to the previous scenario (x = 0.6), the points are shifted upwards, indicating a greater preference for the liquid phase to flow downwards.
Unlike the liquid phase, the vapour phase is again distributed relatively evenly for each mass flux value.

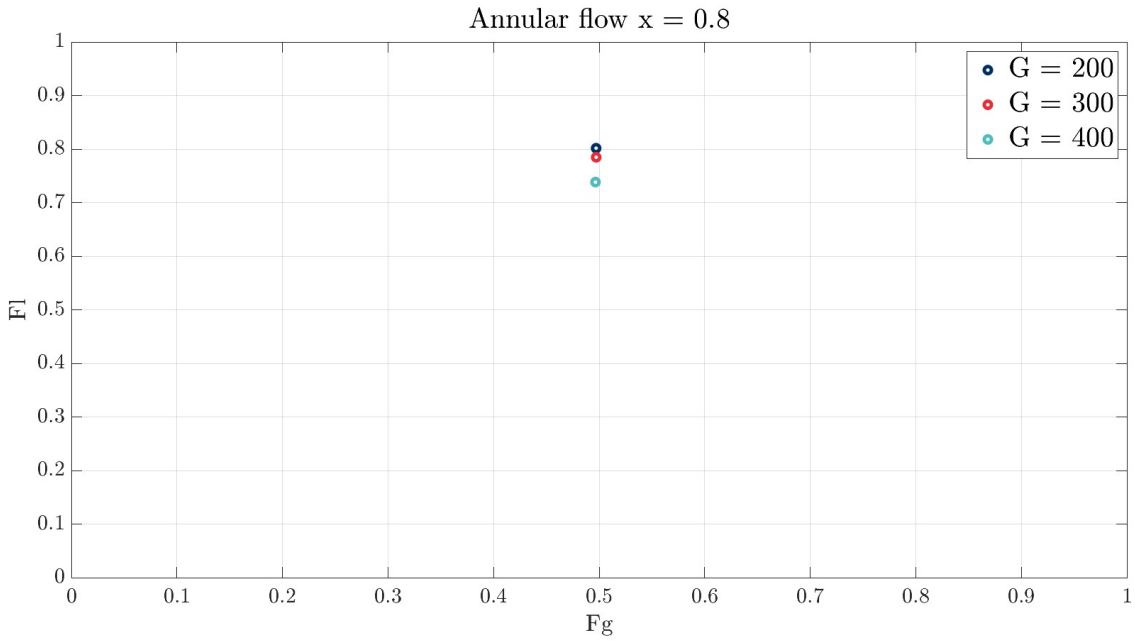

Figure 8.2: Results for annular flows featuring different mass fluxes, with a constant vapour quality of 0.8

The same plot was made for simulations featuring a vapour quality of 0.2, resulting in Figure 8.3, which supports the findings of Figures 8.1 and 8.2.
However, considering a G-value of 300 and 400$\frac{kg}{m^2 s}$, an intermittent flow regime should be obtained based on Figure 7.2. This was not the case, which can be attributed to the relatively short length of the inlet. In order to be able to fully develop an intermittent flow regime a significant inlet length is required. This was not feasible as it would significantly increase the required computational time. Nevertheless, the same trends as for the annular flows are observed, these results are therefore plotted.
Despite the incomplete development of the intermittent/slug flow regime, more liquid and less vapour was carried upwards as the superficial velocity of each phase increased, which supports the findings of Figures 8.1 and 8.2. However, for low G-values a more pronounced maldistribution of the vapour phase was obtained compared to annular flows.

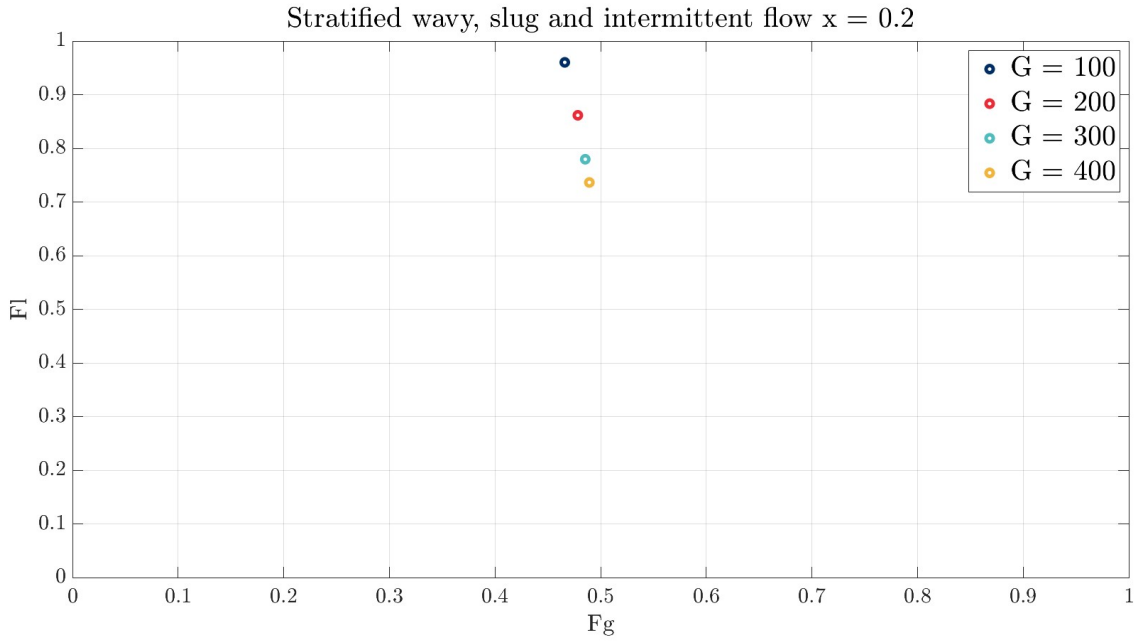

Figure 8.3: Results for flows featuring different mass fluxes, with a constant vapour quality of 0.2

Based on the results described in this section, it became clear that by increasing the mass flux, more liquid was carried into the upper branch. This indicates that increasing the superficial vapour and liquid velocity, which results in increase of the inertial forces, results in a decreasing influence of the gravitational forces. Hence, the findings of Billiet [5], who stated that at higher superficial velocities, the liquid is more dispersed into small droplets upon impact with the wall, is supported. Small droplets are transported more easily compared to larger droplets, thereby decreasing the phase separation. In this way the gravitational forces can be counteracted by the inertial forces, leading to a more even distribution of the two phases.
Menon et al. [21] conducted research on the influence of the superficial velocities in branching T-junctions and found that increasing the superficial liquid velocity leads to more liquid carry-over into the upper branch. This supports the finding that increasing the inertial forces reduces the influence of gravitational forces, resulting in an increasing preference for the liquid of flowing towards the upper outlet.

8.2 Vapour quality

In this section the influence of the vapour quality on the phase separation is investigated for different flow regimes.

In the first scenario, different x-values are plotted for a constant mass flux of $100\frac{kg}{m^2s}$, all of which resulted in a stratified wavy flow regime at the inlet. During the simulation process, almost all of the liquid was carried into the second branch. However, occasionally, droplets were carried into the upper branch. The number of droplets carried into the third branch increased with an increasing vapour quality.
These observations are depicted in Figure 8.4, where the aforementioned trends are clearly visible.

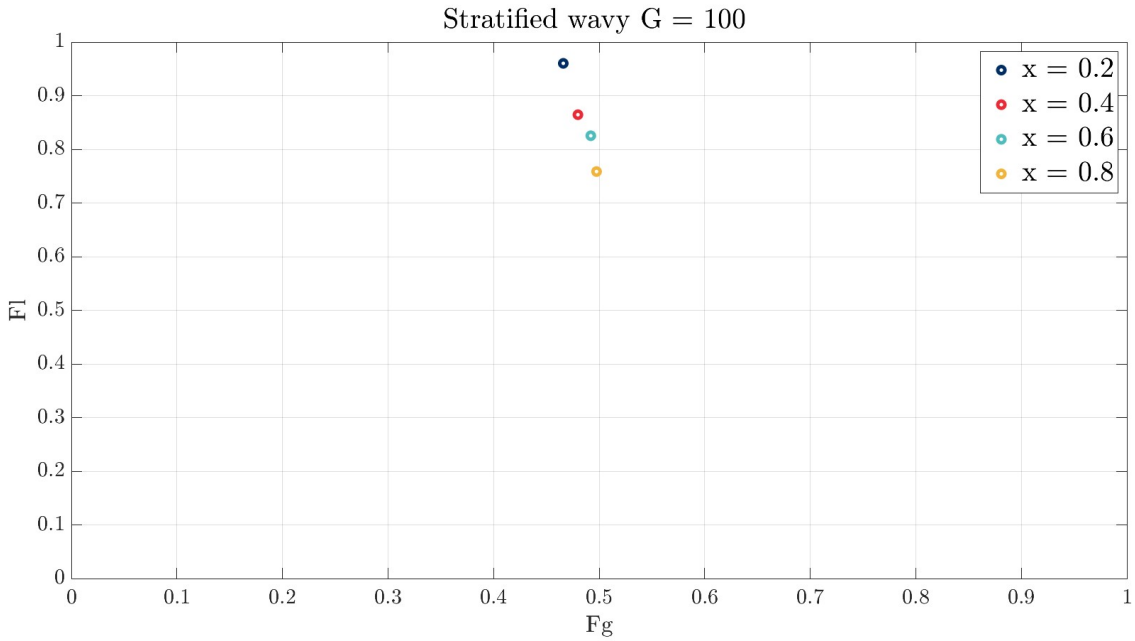

Figure 8.4: Results for stratified wavy flows featuring different vapour qualities, with a constant mass flux of $100\frac{kg}{m^2s}$

The influence of the x-value on the phase separation was also investigated for annular flows featuring different G-values.
Increasing the vapour quality led to an increasing phase separation, causing a preference for the liquid phase to flow towards the lower branch. This trend is depicted on Figures 8.5, 8.6 and 8.7.
Despite the maldistribution of the liquid phase, the vapour phase was consistently distributed evenly across all scenarios, with each point aligning almost perfectly with an Fg-value of 0.5.

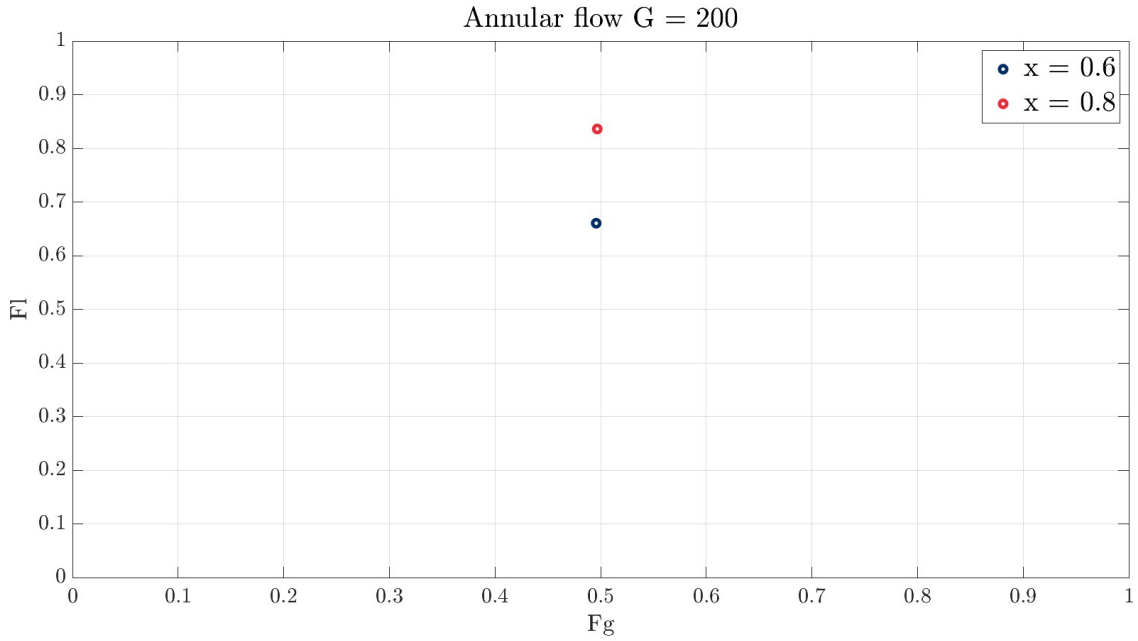

Figure 8.5: Results for annular flows with different vapour qualities, at a constant mass flux of $200 \frac{kg}{m^2 s}$

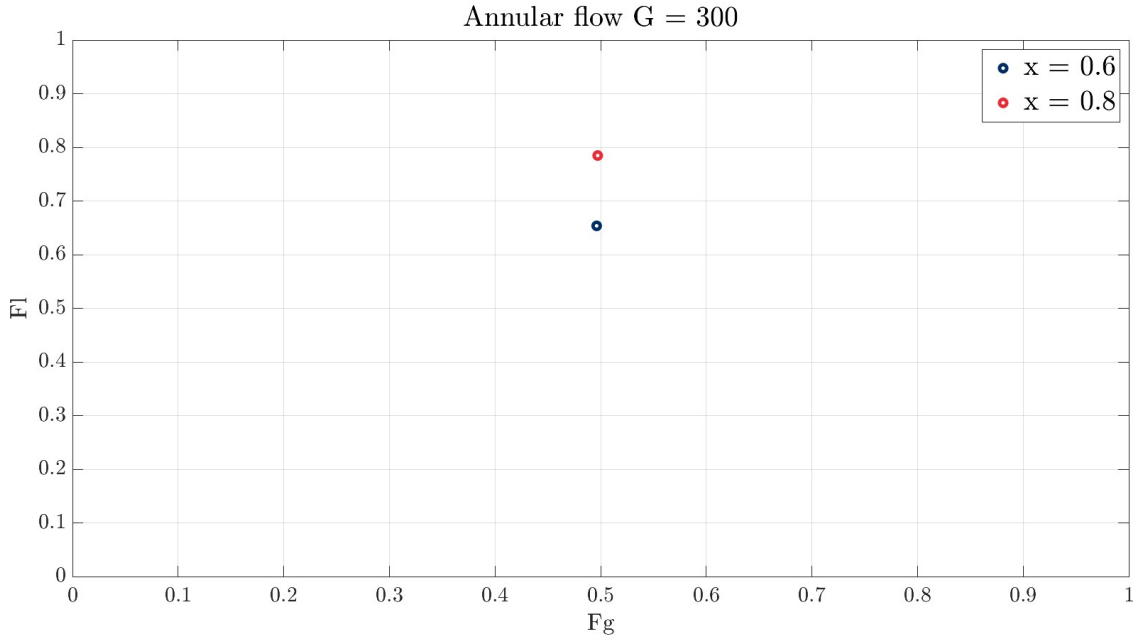

Figure 8.6: Results for annular flows with different vapour qualities, at a constant mass flux of $300 \frac{kg}{m^2 s}$

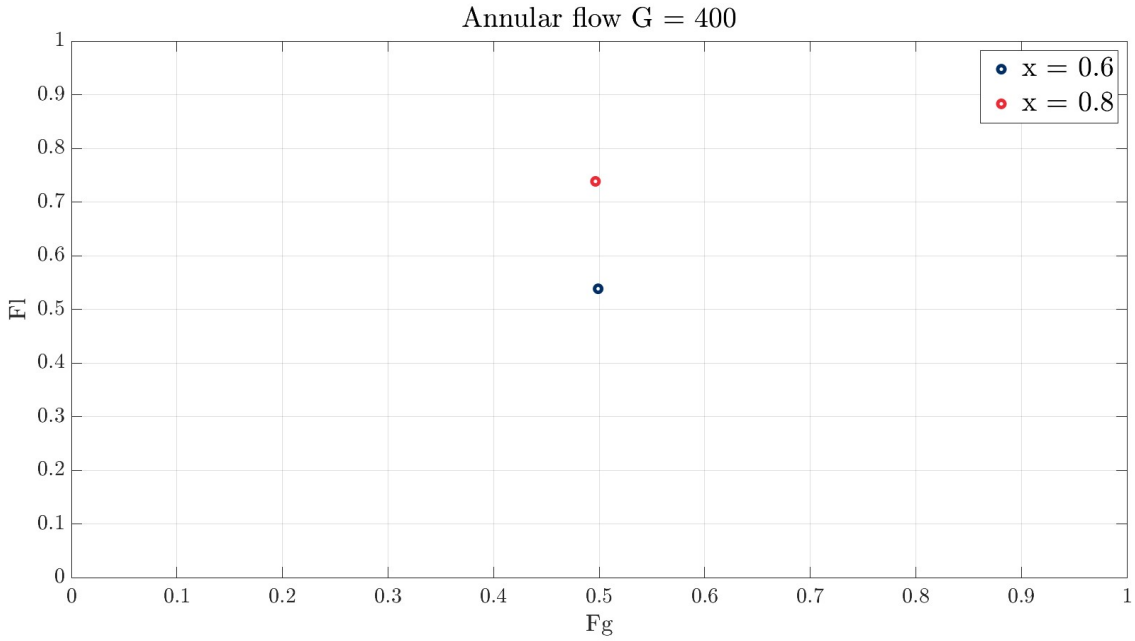

Figure 8.7: Results for annular flows with different vapour qualities, at a constant mass flux of $400 \frac{kg}{m^2 s}$

Based on the results described in this section, the influence of the vapour quality depends on the type of flow regime. For the stratified wavy flows, increasing the vapour quality resulted in a decreasing preference for the liquid of flowing into the lower branch. This is attributed to the maintenance of a constant mass flux ($100 \frac{kg}{m^2 s}$) across the simulations plotted in Figure 8.4, where in order to maintain this mass flux, the velocity of the vapour phase needed to be increased while the liquid velocity was maintained relatively constant (Eq.7.1). Consequently, there was an increased dominance of inertial forces over gravitational forces, which approves the findings found in the literature [5], [21].
However, for the annular flows it was found that increasing the vapour quality resulted in an increasing preference of the liquid to flow downwards, which can be explained by Eq.7.1, where the superficial liquid velocity decreased while the superficial vapour velocity increased in order to maintain the same mass flux. This reduces the droplet formation, resulting in a significant influence of the gravitational force on the maldistribution of the two phases. This finding aligns with the results of Chen et al. [17], who observed a greater influence of superficial liquid velocity compared to superficial vapour velocity. For this reason, the positive influence of an increased superficial vapour velocity on phase distribution is counteracted by the decreasing superficial liquid velocity.

8.3 Different flow regimes

The phase separation results of a certain flow regime depend (among others) on the mass flux and vapour quality, as denoted in section 8.1 and 8.2. Despite these findings, general differences between these flow regimes are still observed.
In general, annular flows are distributed more evenly compared to simulations featuring stratified wavy flows, supporting the findings of Mohamed et al. [22]. This can be attributed to their inherently higher vapour and liquid superficial velocities, which promotes droplet formation after the collision with the wall [5].
Additionally, the physical distribution of phases at the inlet contributes to the enhanced phase distribution of annular flows. With the liquid phase surrounding the vapour phase, the liquid above the annular flow is easily elevated towards the upper outlet by the lower vapour phase. Due to this (more or less) symmetrical nature of the annular flows, the vapour phase is also dragged more easily into the lower branch, where the gravitational forces overrule the inertial forces, resulting in a more even distribution of the vapour phase compared to the stratified wavy flows.
The findings are plotted on Figure 8.8.

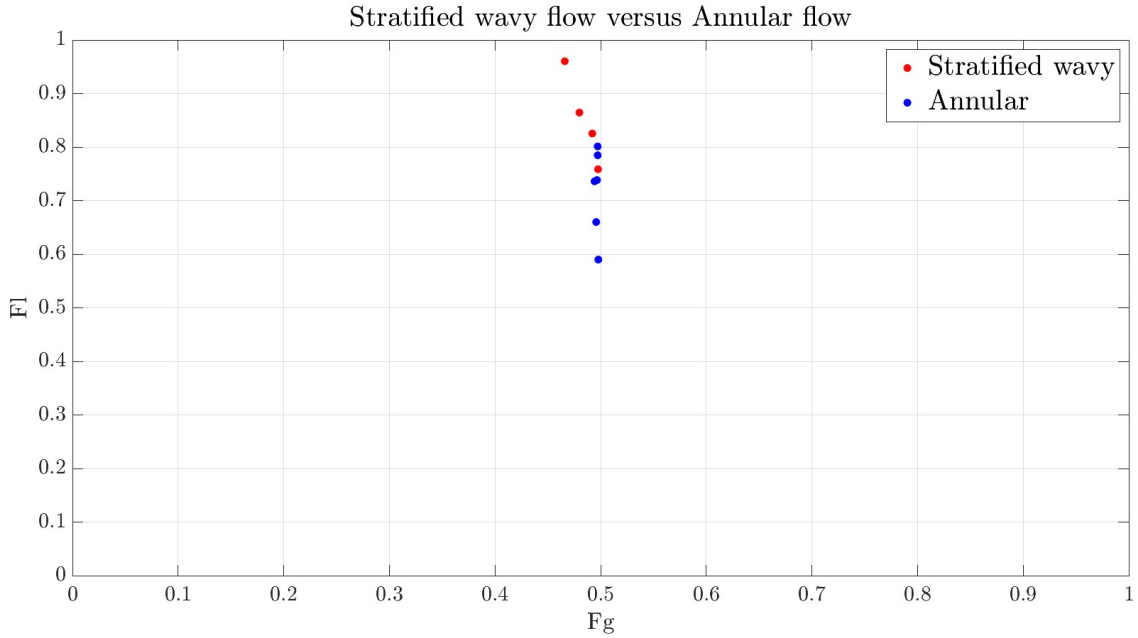

Figure 8.8: Comparison of phase separation: Stratified Wavy Flows vs. Annular Flows

8.4 General comparison with the literature

In this thesis, series of simulations were performed, featuring different vapour qualities and mass fluxes.
Section 3.1 highlighted that based on the mass flux and the vapour quality both the superficial liquid and vapour velocity can be calculated. Consequently, changing the mass flux or vapour quality should change the superficial velocity. Thus, considering the influence of the parameters x and G also involves assessing their impact on the superficial velocity (as discussed in section 3.6.2), which influences the ratio between the inertial and the gravitational forces.
In this way, the findings found in the literature and described in section 3.6.2, found by Billiet [5], Menon et al. [21] and Elazhary et al.[20], were acknowledged by the results obtained from the simulations. These simulations revealed that an increase in superficial velocity, particularly in the liquid phase, led to a reduction in maldistribution. However, increasing the superficial vapour velocity while decreasing the superficial liquid velocity leads to an enlarged maldistribution, which supports the findings of Chen et al. [17].
Overall, especially for the stratified wavy flow regimes, significant maldistribution was observed, which can be attributed to the 90° angle of inclination, supporting the findings of Mohamed et al. [22].

9 Conclusions

During this thesis different flow regimes were simulated in an horizontal T-junction with vertical branches, which represents the manifold of the evaporator of a heat pump.
Based on the flow regime map of Figure 7.2 in combination with Eq.7.1, the physical distribution of the two phases at the inlet was determined. In this way different flow regimes were simulated in an efficient way. However, incomplete development of intermittent and slug flow regimes was observed, attributed to the relatively short inlet length of 55mm, limiting the space available for flow regime development. As a result, flow regimes in which large slugs or bubbles are formed could not fully develop. The complete development of the intermitted flow regimes can be established by enlarging the inlet significantly. Consequently, this will substantially increase the computational time.
Nevertheless, results for annular flows featuring different void fractions and mass fluxes were investigated. The same was done for stratified wavy flows. In this way the influence of the mass flux was investigated for flows featuring vapour qualities of 0.2, 0.6 and 0.8. Furthermore, investigation into the influence of the vapour quality for different flow regimes was performed. This was done for mass flux values of 100, 200, 300 and 400$\frac{kg}{m^2 s}$. Afterwards a more general comparison between the different flow regimes was conducted.

Based on the results obtained by the simulations, it was found that by augmenting the mass flux, the maldistribution of the two phases was reduced. It was also found that for an increasing vapour quality more liquid was carried into the upper branch considering a stratified wavy and intermittent flow regime. Conversely, in annular flows, increasing vapour quality consistently reduced the preference of the liquid to flow towards the upper branch.
These findings were explained by examining the ratio between inertial and gravitational forces, which are influenced by the superficial velocities. These superficial velocities are changed by changing the mass flux and/or the vapour quality.
Following this reasoning, augmenting the mass flux leads to an increase of the superficial velocity of both phases. However, according to Eq.7.1 increasing the vapour quality does not necessarily result in an increase of the superficial liquid velocity. Therefore, different outcomes are observed for increasing vapour quality on the phase separation across different flow regimes.
The trends described above enable the construction of a general statement regarding the influence of occurring flow regimes on phase separation. In this way the annular flow regimes, especially when the mass flux was increased, were found to have a positive influence on the phase distribution.
The results obtained in section 8 approved the finding of the literature (described in section 3.6), where multiple sources approved the positive influence of higher superficial liquid velocity values on the phase distribution.

10 Future work

During this thesis eq.7.1 was used, yielding reasonable results for the void fraction. However, a deviation occurred due to the assumption that the through-averaged velocity in the tube equaled the inlet velocity, which in reality is only an approximation. Consequently, the tested values for the vapour quality and mass flux dit not precisely align with the intended parameters. Nevertheless, by selecting the intended values sufficient distant from transitional flow regimes, the desired trends where not affected.

In order to be able to avoid this deviation, an iterative approach is necessary. In which, simulations need to be executed in order to detemine the averaged velocity based on the inlet velocity. However, this method is time-consuming.
For this reason, future work should aim to find an alternative for this iterative approach.

A: Pictures of the Model

Figure A1: Simulation result showing a stratified wavy flow

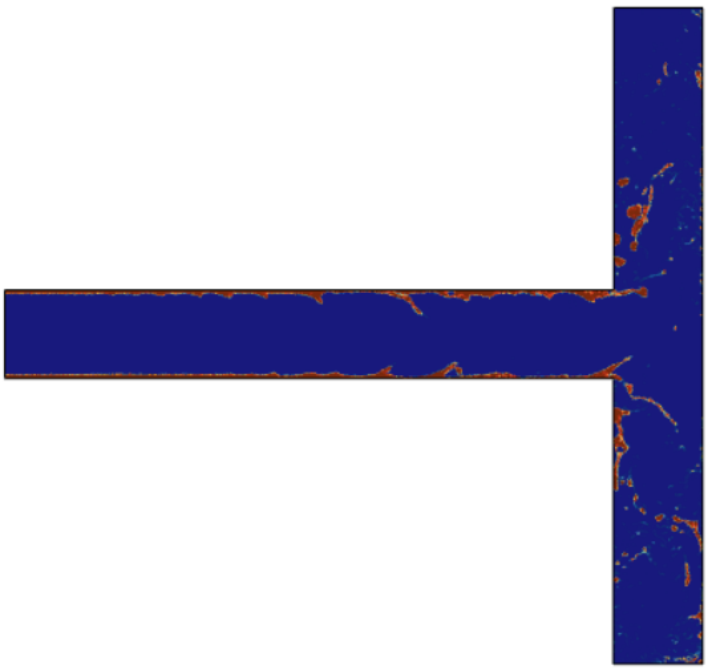

Figure A2: Simulation result showing an annular flow

Bibliography

[1] Jong Min Choi, W Vance Payne, and Piotr A Domanski. "Effects of non-uniform refrigerant and air flow distributions on finned-tube evaporator performance". In: *International Congress Refrigeration*. Citeseer. 2003.

[2] Martin Wörner. *A compact introduction to the numerical modeling of multiphase flows*. Vol. 6932. FZKA, 2003.

[3] EV Rebrov. "Two-phase flow regimes in microchannels". In: *Theoretical foundations of chemical engineering* 44.4 (2010), pp. 355–367.

[4] Jorge MORENO. "Experimental and analytical study of two-phase pressure drops during evaporation in horizontal tubes". In: *Ecole Polytechnique Federale de Laussane. France. Docteur These* (2005).

[5] Marijn Billiet. "Phase distribution of a refrigerant two-phase flow over an impacting T-junction". PhD thesis. Ghent University, 2018.

[6] Fahad Matovu, JM Heinz Preisig, and John Morud. "Drift-flux models". In: (2014).

[7] Omar Ahmed Mohamed Abdelhamid Elshawarby. "Computational fluid dynamics of multiphase flow using ANSYS fluent". In: (2020).

[8] Lixin Cheng. *Frontiers and progress in multiphase flow I*. Springer, 2014.

[9] P Barbieri, J Jabardo, E Bandarra Filho, et al. "Flow patterns in convective boiling of refrigerant R-134a in smooth tubes of several diameters". In: *Proceedings of the 5th European Thermal-Sciences Conference, Eindhoven, The Netherlands*. Citeseer. 2008, pp. 18–22.

[10] MK Akbar, DA Plummer, and S Mlip Ghiaasiaan. "On gas–liquid two-phase flow regimes in microchannels". In: *International Journal of Multiphase Flow* 29.5 (2003), pp. 855–865.

[11] Hugo Canière et al. "Mapping of horizontal refrigerant two-phase flow patterns based on clustering of capacitive sensor signals". In: *International Journal of Heat and Mass Transfer* 53.23-24 (2010), pp. 5298–5307.

[12] Wanchun Sun et al. "The phase distribution of gas-liquid two-phase flow in microimpacting T-junctions with different branch channel diameters". In: *Chemical Engineering Journal* 333 (2018), pp. 34–42.

[13] MA Mohamed, HM Soliman, and GE Sims. "Effects of pipe size and system pressure on the phase redistribution in horizontal impacting tee junctions". In: *Experimental Thermal and Fluid Science* 54 (2014), pp. 219–224.

[14] S T Hwang, H M Soliman, and RT Lahey Jr. "Phase separation in impacting wyes and tees". In: *International Journal of Multiphase Flow* 15.6 (1989), pp. 965–975.

[15] Marcel Ottens et al. "Gas-liquid flow splitting in regular, reduced and impacting T junctions". In: *Impianistica Italiana* 8 (1995).

[16] Jinfang Chen et al. "Experimental investigation of annular two-phase flow splitting at a microimpacting T-junction". In: *Chemical Engineering Science* 118 (2014), pp. 154–163.

[17] Jinfang Chen et al. "Experimental investigation of two-phase slug flow splitting at a micro impacting T-junction". In: *International Journal of Heat and Mass Transfer* 81 (2015), pp. 939–948.

[18] Faheem Ejaz, William Pao, and Mohammad Shakir Nasif. "Review of factors affecting the phase-redistribution in the branching T-junction". In: *Journal of Advanced Research in Fluid Mechanics and Thermal Sciences* 84.1 (2021), pp. 60–77.

[19] AMF El-Shaboury, HM Soliman, and GE Sims. "Two-phase flow in a horizontal equal-sided impacting tee junction". In: *International journal of multiphase flow* 33.4 (2007), pp. 411–431.

[20] AM Elazhary and HM Soliman. "Two-phase flow in a horizontal mini-size impacting T-junction with a rectangular cross-section". In: *International journal of multiphase flow* 42 (2012), pp. 104–114.

[21] Zeeshan Qadir Memon et al. "Experimental investigation of two-phase separation in T-Junction with combined diameter ratio". In: *Journal of Natural Gas Science and Engineering* 73 (2020), p. 103048.

[22] MA Mohamed, HM Soliman, and GE Sims. "Experimental investigation of two-phase flow splitting in an equal-sided impacting tee junction with inclined outlets". In: *Experimental thermal and fluid science* 35.6 (2011), pp. 1193–1201.

[23] MA Mohamed, HM Soliman, and GE Sims. "Conditions for complete phase separation in an impacting tee junction at various inclinations of the outlet arms". In: *International Journal of Multiphase Flow* 47 (2012), pp. 66–72.

[24] R Balasubramaniam et al. "Two phase flow modeling: Summary of flow regimes and pressure drop correlations in reduced and partial gravity". In: (2006).

[25] G Das, PK Das, and BJ Azzopardi. "The split of stratified gas–liquid flow at a small diameter T-junction". In: *International journal of multiphase flow* 31.4 (2005), pp. 514–528.

[26] A Azzi et al. "Gas–liquid two-phase flow division at a micro-T-junction". In: *Chemical engineering science* 65.13 (2010), pp. 3986–3993.

[27] Stefan Radl and Federico Municchi. "Spatial filtering for scale bridging and its application to transport in dense particle beds". In: *Advances in Chemical Engineering*. Vol. 53. Elsevier, 2018, pp. 153–237.

[28] R Silva et al. "Evaluating the performance of the mixture model coupled with high and low Reynolds turbulence closures in the numerical description of concentrated solid-liquid flows of settling particles". In: *The Journal of Computational Multiphase Flows* 7.4 (2015), pp. 241–257.

[29] ANSYS. *Overview and Limitations of the Eulerian Model*. 23/04/2024. 2009-01-23. URL: `https://www.afs.enea.it/project/neptunius/docs/fluent/html/th/node320.htm`.

[30] Renato Soccol et al. "Numerical analysis of the interphase forces in bubble columns using euler-euler modelling framework". In: *The Canadian Journal of Chemical Engineering* 93.11 (2015), pp. 2055–2069.

[31] Marianne Sjöstrand. *CFD simulations of two-phase flows passing through a distributor*. Chalmers University of Technology, 2008.

[32] Shahab Mirjalili, Suhas S Jain, and Micheal Dodd. "Interface-capturing methods for two-phase flows: An overview and recent developments". In: *Center for Turbulence Research Annual Research Briefs* 2017.117-135 (2017), p. 13.

[33] Kurian J Vachaparambil and Kristian Etienne Einarsrud. "Comparison of surface tension models for the volume of fluid method". In: *Processes* 7.8 (2019), p. 542.

[34] Mark Sussman, Peter Smereka, and Stanley Osher. "A level set approach for computing solutions to incompressible two-phase flow". In: *Journal of Computational physics* 114.1 (1994), pp. 146–159.

[35] M García et al. "Evaluation of Euler-Euler and Euler-Lagrange strategies for large-eddy simulations of turbulent reacting flows". In: *ECCOMAS thematic conference on computational combustion*. Vol. 30. 2005, pp. 1–18.

[36] Tony Persson. "Eulerian-Lagrangian Modeling of Multicomponent Spray for Aseptic Treatment of Carton Bottles in the Food Process and Packaging Industry". In: (2013).

[37] P Durbin and TIP Shih. "An overview of turbulence modeling". In: *Modelling and Simulation of Turbulent Heat Transfer* 16.3 (2005).

[38] BJ Azzopardi, A Purvis, and AH Govan. *Flow split of churn flow at a vertical impacting T, UKAEA Report*. Tech. rep. AERE, 1986.

[39] B J Azzopardi, A Purvis, and AH Govan. "Annular two-phase flow split at an impacting T". In: *International journal of multiphase flow* 13.5 (1987), pp. 605–614.

[40] Sze-Foo Chien and Mark T Rubel. "Phase splitting of wet steam in annular flow through a horizontal impacting tee". In: *SPE production engineering* 7.04 (1992), pp. 368–374.

[41] Sze-Foo Chien. "Phase splitting of wet steam in annular flow through a horizontal branching tee". In: *SPE Production & Facilities* 11.02 (1996), pp. 83–88.

[42] K C Hong and Suzanne Griston. "Two-phase flow splitting at an impacting tee". In: *SPE Production & Facilities* 10.03 (1995), pp. 184–190.

[43] Nanami Kishida Yoji Onoaka Rihito Adachi and Takashi Matsumoto. "Prediction Model of Two-Phase Flow Distribution in a Vertical Header". In: *International Congress of Refrigeration* (2023), pp. 237–248.

[44] Pei Lu et al. "Simulation of two-phase refrigerant separation in horizontal T-junction". In: *Applied Thermal Engineering* 134 (2018), pp. 333–340.

[45] Minh Tran et al. "Numerical simulation of two-phase separation in T-junction with experimental validation". In: *Journal of Mechanical Engineering and Sciences* 12.4 (2018), pp. 4216–4230.

[46] American Society of Mechanical Engineers. Fluids Engineering Division. *Quantification of Uncertainty in Computational Fluid Dynamics*. American Society of Mechanical Engineers, 1993.

[47] DM Graham. "Experimental investigation of void fraction during refrigerant condensation". In: *Air Conditioning and Refrigeration Center TR-135* (1997).

[48] Hugo Caniere. "Flow pattern mapping of horizontal evaporating refrigerant flow based on capacitive void fraction measurements". PhD thesis. Ghent University, 2009.